Evolution, 57(8), 2003, pp. 1900–1916

PHYLOGEOGRAPHY AND INTROGRESSIVE HYBRIDIZATION: CHIPMUNKS (GENUS *TAMIAS*) IN THE NORTHERN ROCKY MOUNTAINS

JEFFREY M. GOOD,[1,2] JOHN R. DEMBOSKI,[3] DAVID W. NAGORSEN,[4,5] AND JACK SULLIVAN[1]
[1]*Department of Biological Sciences, Box 443051, University of Idaho, Moscow, Idaho 83844-3051*
[3]*Biological Sciences Department, California State Polytechnic University, Pomona, 3801 West Temple Avenue, Pomona, California 91768-4032*
[4]*Royal British Columbia Museum, Victoria, British Columbia V8V 1X4, Canada*

Abstract.—If phylogeographic studies are to be broadly used for assessing population-level processes relevant to speciation and systematics, the ability to identify and incorporate instances of hybridization into the analytical framework is essential. Here, we examine the evolutionary history of two chipmunk species, *Tamias ruficaudus* and *Tamias amoenus*, in the northern Rocky Mountains by integrating multivariate morphometrics of bacular (os penis) variation, phylogenetic estimation, and nested clade analysis with regional biogeography. Our results indicate multiple examples of mitochondrial DNA introgression layered within the evolutionary history of these nonsister species. Three of these events are most consistent with recent and/or ongoing asymmetric introgression of mitochondrial DNA across morphologically defined secondary contact zones. In addition, we find preliminary evidence where a fourth instance of nonconcordant characters may represent complete fixation of introgressed mitochondrial DNA via a more ancient hybridization event, although alternative explanations of convergence or incomplete sorting of ancestral polymorphisms cannot be dismissed with these data. The demonstration of hybridization among chipmunks with strongly differentiated bacular morphology contradicts long-standing assumptions that variation within this character is diagnostic of complete reproductive isolation within *Tamias*. Our results illustrate the utility of phylogeographic analyses for detecting instances of reticulate evolution and for incorporating this and other information in the inference of the evolutionary history of species.

Key words.—Bacula, Bayesian phylogeny, hybrid zone, introgression, multivariate morphometrics, nested clade analysis.

Received June 12, 2002. Accepted April 16, 2003.

The concept of biological species existing as genetically cohesive populations has been central to the study of animal speciation since the modern synthesis (Dobzhansky 1950; Mayr 1963). Therefore, analyzing spatial subdivision within and among species at geographic zones of hybridization may provide a unique opportunity to understand mechanisms of reproductive isolation and speciation in nature (Hewitt 1989). Insight into the process and spatial pattern of natural hybridization has been greatly advanced by the application of cline theory (Rieseberg et al. 1999; Barton 2001; Brumfield et al. 2001). Character distributions across a zone of hybridization are often geographically coincident in cline shape and width, suggesting a balance between dispersal and selection within the zone (Haldane 1948; Barton and Hewitt 1985). However, one interesting deviation occurs when one or a few characters exhibit asymmetric introgression beyond the contact zone (Anderson 1949). This phenomenon has been established for a number of hybridizing animal taxa (Dowling and Hoeh 1991; Jaarola et al. 1997; Sota et al. 2001; Ross and Harrison 2002) and is often characterized by differential movement of mitochondrial DNA (mtDNA) relative to nuclear and/or morphological markers (Wirtz 1999).

Nevertheless, detection and analysis of such events can be problematic. In particular, extensive introgressive hybridization can be difficult to differentiate from incomplete sorting of ancestral polymorphisms as an explanation of nonconcordant character sets across related taxa (Harrison and Bogdanowicz 1997; Goodman et al. 1999; Hare et al. 2002). Furthermore, the temporal distribution of potentially hybridizing taxa may be quite fluid, which could result in evolutionarily layered patterns of hybridization that obscure differentiation between historical and contemporary character introgression (Arntzen and Wallis 1991). In such instances, historical biogeography and phylogeographic data may provide a means to differentiate introgression from retention of ancestral polymorphisms. For phylogeographic data to be useful in this context, the associations of nonconcordant characters must be framed within a geographic context. One method that may be useful for establishing statistical associations of both observed phenotypes and geography with genealogical structure is nested clade analysis (NCA; Templeton and Sing 1993; Templeton et al. 1995). In general, NCA has been used to evaluate the cohesion of evolutionary lineages (Wiens and Penkrot 2002), even when hybridization is among the potential population processes contributing to the geographic structuring of genetic variation (Templeton 1994; Matos and Schaal 2000).

Chipmunks (*Tamias*) of western North America represent a mammalian group whose radiation, evolutionary relationships, and biogeographic history appear to be particularly complex (Patterson 1982; Good and Sullivan 2001; Piaggio and Spicer 2001; Demboski and Sullivan 2003). Two processes are thought to be most relevant to speciation and diversification within this group. First, species of western chipmunks are strongly associated with distinct ecological communities (Johnson 1943), suggesting differential environmental adaptations. As a result, western chipmunks are often distributed as a mosaic of parapatric species partitioned by

[2] Present address: Department of Ecology and Evolutionary Biology, University of Arizona, Biosciences West, Tucson, Arizona 85721; E-mail: jgood@email.arizona.edu.
[5] Present address: Mammalia Biological Consulting, 4268 Metchosin Road, Victoria, British Columbia V9C 3Z4, Canada.

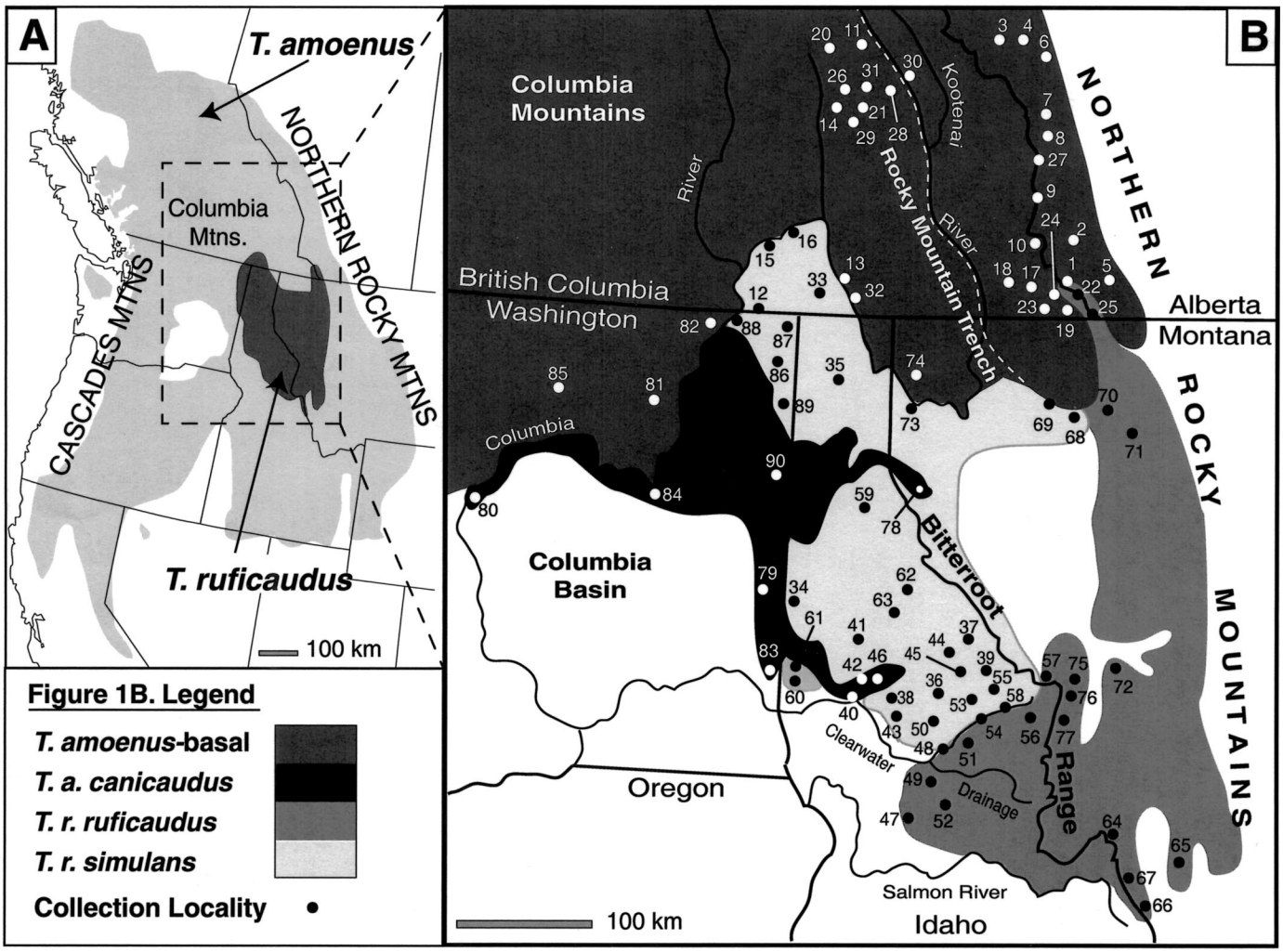

FIG. 1. (A) Distribution of *Tamias ruficaudus* and *Tamias amoenus* in western North America as modified from Hall (1981). (B) Our working hypothesis of the geographic distribution of the five taxonomic units examined in this study (see text). More detailed sampling and locality information is given in the Appendix. To avoid confusion, data regarding nonfocal *T. amoenus* occurring within this region are not shown. This information is available in Demboski and Sullivan (2003).

habitat preference and interspecific competition (Brown 1971; Chappell 1978). Second, strong differentiation in genital morphology is thought to contribute to reproductive isolation via a lock-and-key mating system (Patterson and Thaeler 1982). Divergence in genitalia is most pronounced in the male genital bone, the baculum or os penis, which tends to be highly variable among chipmunk species yet exhibits low intraspecific variation (White 1953; Callahan 1977; Sutton and Patterson 2000). Indeed, one striking aspect of western chipmunk diversification is the relatively unambiguous recognition of all 23 currently described species based on bacular differentiation (White 1953; Sutton and Patterson 2000).

This study focuses on identifying patterns of hybridization between two codistributed chipmunk species that exhibit both characteristic ecological niche partitioning and strong bacular differentiation. The distribution of the red-tailed chipmunk, *Tamias ruficaudus*, is completely nested within the geographic range of the widespread yellow-pine chipmunk, *Tamias amoenus*, in the northern Rocky Mountains (Fig. 1A). Within this region, *T. ruficaudus* is typically found at higher elevations in dense, mesic forests, whereas *T. amoenus* tends to occupy lower-elevation, xeric forests (Howell 1929; Hoffmann and Pattie 1968), resulting in extensive regions of parapatry along ecological transitions (Best 1993). These species are not sister taxa, and each belongs to a separate species group within *Tamias* that may span the deepest phylogenetic divergence among species of western chipmunks (Piaggio and Spicer 2001; Demboski and Sullivan 2003).

Pronounced bacular differentiation has previously been described between *T. amoenus* and *T. ruficaudus* (White 1953; Sutton 1992). In addition, distinct bacular morphology has been identified between the two subspecies within *T. ruficaudus*, *T. r. ruficaudus* and *T. r. simulans*, leading some authors to postulate that they may be reproductively isolated species (Patterson and Heaney 1987). Conversely, a recent phylogeographic study in *T. ruficaudus* (Good and Sullivan 2001) reported patterns of mtDNA variation consistent with gene flow across two bacular contact zones between *T. r. ruficaudus* and *T. r. simulans*. Furthermore, preliminary mtDNA analyses indicate that one subspecies of *T. amoenus*,

T. a. canicaudus, is phylogenetically nested within the nonsister *T. ruficaudus* clade (Good and Sullivan 2001; Demboski and Sullivan 2003).

The objectives of this study are to expand upon the findings of Good and Sullivan (2001) and Demboski and Sullivan (2003) by integrating multivariate morphometrics, phylogenetics, and NCA into an examination of phylogeography and introgressive hybridization between *T. ruficaudus* and *T. amoenus*. Phylogenetic relationships estimated from mtDNA sequences, bacular variation based on multivariate analyses, and a priori taxonomic hypotheses are compared within and between *T. ruficaudus* and *T. amoenus* to assess the degree of concordance among these data. The permutation tests inherent to NCA are used to examine the association of haplotype structure with both geography and morphology. Phylogeographic patterns of nonconcordance are then evaluated within the context of regional biogeographic history to differentiate, when possible, between incomplete sorting of ancestral polymorphisms and contemporary and/or historical introgressive hybridization.

Materials and Methods

Taxonomic Sampling

We examined molecular and/or morphological data from 420 specimens (males and females) of *T. ruficaudus* and *T. amoenus* sampled from 90 locations where the two species are codistributed (Fig. 1B, Appendix). The shaded ranges in Figure 1B represent our working hypothesis of the geographic distribution of the five taxonomic units examined in this study. These were synthesized from available phenotypic (Hall 1981; Patterson and Heaney 1987; D. W. Nagorsen, unpubl. data) and molecular data (Good and Sullivan 2001; Demboski and Sullivan 2003) as well as established habitat associations (Sutton 1992; Best 1993). In regions where taxonomic distributions were unclear due to previously reported discrepancies among characters, we set limits corresponding to potential geographic dispersal barriers. Given obvious discrepancies between current subspecific *T. amoenus* taxonomy (Sutton 1992), observed patterns of genetic variation (Demboski and Sullivan 2003), and genital bone morphology (D. W. Nagorsen, unpubl. data) in this region, we delimited the three *T. amoenus* taxonomic units used in this study as follows. Specimens of *T. a. canicaudus* were determined to be those individuals that possessed the distinct pelage diagnostic of this taxon (Merriam 1903) and sampled from within the distribution delimited by Hall (1981). Specimens distributed in this region currently classified as *T. a. affinis* and *T. a. luteiventris* represent a highly divergent basal mtDNA assemblage of *T. amoenus* (>7% uncorrected cytochrome *b* sequence divergence from other *T. a. luteiventris* and *T. a. affinis*; Demboski and Sullivan 2003). Within this basal clade, populations occurring in the Rocky Mountains east of the Rocky Mountain Trench (a geographical barrier, see Fig. 1) possess distinct male and female genital bone morphology relative to those sampled from various minor ranges on the western slope of the Rocky Mountain formation (D. W. Nagorsen, unpubl. data), which are collectively referred to as the Columbia Mountains. Therefore, these two taxa will be referred to as *T. amoenus*-basal Rocky Mountains (RM) and *T. amoenus*-basal Columbia Mountains (CM) throughout this analysis.

Morphometric Data Collection and Analyses

We examined 203 cleared and stained bacula of males sampled from 77 localities (see Appendix). We recorded five measurements from each specimen: shaft length, tip length, tip angle, keel height, and base width (Sutton and Nadler 1974; Patterson 1982). For all specimens collected in Canada, distance measurements were taken directly with a stereomicroscope (20×) and an ocular micrometer, whereas tip angle was measured with a protractor from camera lucida projections. Specimens from all other locations were photographed (ventral and right lateral aspects) at approximately 40× with a camera mounted on a M5 stereomicroscope. Digitized images were individually calibrated using known in-screen distances and were measured using MacMorph version 2.1 (Spencer and Spencer 1994). To account for ontogenetic variation, specimens were classified into three age categories (juveniles, subadults, and adults) based on patterns of maxillary dentition (Beg and Hoffman 1977). Subadults and adults were pooled in morphometric analyses because the baculum has been repeatedly shown to obtain adult dimensions relatively early in development (White 1953; Adams and Sutton 1968; Beg and Hoffman 1977). Juveniles and specimens of unknown age (skull damaged or absent) were examined for classification purposes only ($n = 29$, see below).

All morphometric analyses were conducted with SYSTAT 10 (Systat Software, Inc., Richmond, CA). Adult and subadult samples were partitioned, a priori, into the five taxonomic groups delimited in Figure 1B. Due to sampling restrictions, within-group geographic variation was not examined. For each group we calculated standard univariate statistics and compared means with a one-way ANOVA. Post hoc comparisons of means were conducted with Tukey's studentized range statistic to account for multiple comparisons. In addition, bacular variation was assessed using a MANOVA, a five-group linear discriminant function analysis, a principle components analysis (PCA; a priori taxonomic groups were not assumed for this analysis), and a canonical variate analysis (CVA). Classification ability of linear functions was assessed using a jackknife procedure (Lance et al. 2000) and a randomized cross-validation procedure (Orthmeyer et al. 1995), with approximately 0.65 of the group used to estimate a linear function with which the residual test sample was identified. All individuals, including ungrouped juveniles and specimens of unknown age, were classified based on their generalized statistical distance (Mahalanobis' D^2; Mahalanobis 1936) and the corresponding posterior probability of group membership (Reyment et al. 1984).

Molecular Data Collection

Tissue extractions were conducted using two methods. Total genomic DNA was extracted from approximately 10 mg of liver tissue using a CTAB/DTAB protocol (Gustincich et al. 1991). Suboptimal genomic DNA (i.e., from degraded tissues or museum study skins) was extracted using a DNeasy Tissue Kit (Qiagen, Valencia, CA) in a separate facility to avoid

contamination from high-copy DNA sources. For most samples, an approximately 800-bp fragment was amplified from the 5′ end of the mitochondrial cytochrome *b* gene (cyt *b*). Primers were as follows: L-14115: 5′-GATATGAAAAACCATCGTTG-3′; L-14553: 5′-CTACCATGAGGACAAATATC-3′ (Kocher et al. 1989; Sullivan et al. 2000); L-14623: 5′-TCTACTAGTGTTGTTCCGATGTATGG-3′ (Demboski and Sullivan 2003); H-14899: 5′-TCTGGGTCTCCAAGGAGGT-3′ (Good and Sullivan 2001); H-14963: 5′-GGCAAATAGGAARTATCATT-3′ (Kocher et al. 1989; Sullivan et al. 2000). Primer numbers refer to positions in the *Mus* mitochondrial genome (Bibb et al. 1981). The internal primers were used to amplify suboptimal samples, and primers L-14623 and H-14899 were designed specifically for chipmunks. Polymerase chain reaction (PCR) products were purified using polyethylene glycol precipitation or Qiagen QIAquick spin columns and sequenced using a Big Dye Kit (Applied Biosystems, Foster City, CA). Sequencing reactions were optimized using 15–45 ng of PCR product then reduced to 5–25 ng of product per 10-μl reaction for subsequent reactions. A subset of samples was sequenced in only one direction with primer L-14115 to identify major mtDNA type. All sequencing products were filtered using 5% Sephadex G-50 in CentriSep spin columns (Princeton Separations, Adelphia, NJ) and run on an ABI 377 automated sequencer (Applied Biosystems, Inc.) using 4% Long Ranger gels. Sequence data were edited and aligned using Sequencher, version 3.0 (Gene Codes Corp., Ann Arbor, MI). New sequences generated for this study are available on Genbank under the accession numbers AY211770–AY211878.

Phylogenetic Analyses

We examined cyt *b* sequence variation with three separate phylogenetic analyses, using a combination of maximum parsimony performed with PAUP* version 4.0b8–10 (Swofford 2000) and Bayesian estimation performed with MrBayes version 2.1 (Huelsenbeck and Ronquist 2001). An objectively determined model of nucleotide substitution was selected based on likelihood-ratio tests of goodness of fit among 16 alternative models of sequence evolution (see Sullivan et al. 1997) using a χ^2 approximation of the null distribution (Yang et al. 1995).

Bayesian analyses were conducted with random starting trees, run 5.0×10^6 generations and sampled every 100 generations. Base frequencies were estimated directly from the data, whereas initial starting point values for specific nucleotide substitution model parameters were estimated from the data using an equally weighted parsimony tree (arbitrarily chosen). In all searches, stationarity of the Markov chain was determined as the point when sampled log likelihood values plotted against generation time reached a stable mean equilibrium value; burn-in data sampled from generations preceding this point were discarded (Huelsenbeck and Ronquist 2001). All data collected at stationarity were used to estimate posterior nodal probabilities, mean log likelihood scores, and a summary phylogeny including Bayesian estimates of branch lengths. Two independent replicates were conducted and inspected for consistency to check for local optima (Huelsenbeck and Imennov 2002).

In the first analysis, an alignment of 701 bp of cyt *b* for 349 individuals was analyzed. This included 319 specimens sampled from the five focal taxa, as well as major intraspecific clade structure within *T. amoenus* ($n = 9$; Demboski and Sullivan 2003) and a subset of nonfocal chipmunk species ($n = 21$). To ease computational demands, we condensed the data matrix to include only unique haplotypes ($n = 97$) using COLLAPSE version 1.1 (Posada 1999) and performed a Bayesian estimation of the phylogeny with MrBayes version 2.1 (Huelsenbeck and Ronquist 2001). This analysis was conducted to examine the geographic concordance between mtDNA variation and our a priori taxonomic hypotheses in all samples (male and female) for which we had sequence data.

To provide a more direct assessment of the relationship between bacula and mtDNA, we then pruned the 349 dataset to males of known bacular type ($n = 128$, including juveniles). Because this dataset included many examples of individuals with identical sequences, this analysis was restricted to equally weighted parsimony (heuristic search, 10 random addition sequences, tree bisection-reconnection branch swapping). We then mapped bacular morphotypes onto the terminals. Ten specimens were included in this analysis that were not directly analyzed in our morphometric study but were unambiguously classified as *T. r. ruficaudus* in a previous study by Patterson and Heaney (1987) using a similar multivariate approach. Nodal support for this topology was estimated with a parsimony bootstrap (heuristic search, 500 replicates, MAXTREES = 100).

Finally, an alignment of 350 bp was used to assign individuals ($n = 48$) to major mtDNA clades as defined by the previous searches. This analysis was employed to expand sampling and provide a cursory inspection for potential introgression in geographic regions away from identified zones of contact.

Nested Clade Analyses

The resolution of NCA deteriorates with increasing divergence (Templeton et al. 1992); therefore, we restricted our analysis to 701-bp sequences of cyt *b* within clade 2 ($n = 288$; see Results and Fig. 3). We used TCS version 1.13 (Clement et al. 2000) to evaluate the limits of parsimony (Templeton et al. 1992; Posada and Crandall 2001). This provided an estimate of 95% plausibility networks within the dataset that were then hierarchically nested following standard methodology (Templeton et al. 1987; Crandall and Templeton 1993; Templeton and Sing 1993; Castelloe and Templeton 1994; Crandall 1996). Interconnections among plausibility networks were then estimated from a pairwise matrix based on absolute number of differences generated with PAUP* version 4.0b8 (Swofford 2000). Once all networks were interconnected, a separate Bayesian phylogenetic analysis was conducted (as above) to estimate posterior probabilities of nodes associated with these connections. We then proceeded with the hierarchical nesting algorithm by grouping clades united by Bayesian posterior probabilities of $P = 0.95$ or higher.

TABLE 1. Bacular measurements (mean ± standard deviation) for three groups within *Tamias amoenus* and the two subspecies comprising *T. ruficaudus* sampled from a subset of the localities in Figure 1B (see Appendix). All linear measurements are in millimeters and angles are in degrees. Asterisks indicate rejection of the null hypothesis of equal means ($P < 0.001$) when analyzed with one-way ANOVA. Pairwise comparisons of equality of group subsets were assessed using Tukey's studentized range statistic; only nonsignificant ($P > 0.05$) subsets are given. The distributions of measurements within all a priori groupings were not significantly skewed.

Measurement	*T. a. canicaudus* (1)	*T. amoenus*-basal CM (Columbia Mts.; 2)	*T. amoenus*-basal RM (Rocky Mts.; 3)	*T. r. ruficaudus* (4)	*T. r. simulans* (5)	Nonsignificant group subsets
N	26	28	15	35	70	
Shaft length*	2.51 ± 0.10	2.50 ± 0.19	2.69 ± 0.11	4.36 ± 0.20	3.55 ± 0.16	1/2
Tip length*	0.86 ± 0.04	0.90 ± 0.06	0.94 ± 0.06	1.54 ± 0.08	1.60 ± 0.08	1/2, 2/3
Tip angle*	118.68 ± 2.79	120.7 ± 3.08	134.4 ± 3.78	122.0 ± 2.6	119.3 ± 3.0	1/2, 1/5, 2/4, 2/5
Keel height*	0.27 ± 0.03	0.32 ± 0.04	0.32 ± 0.03	0.48 ± 0.03	0.54 ± 0.05	2/3
Basal width*	0.58 ± 0.05	0.55 ± 0.04	0.48 ± 0.05	0.80 ± 0.07	0.91 ± 0.09	1/2

Significant associations of categorical variables (both sampling localities and bacular morphotypes) were assessed hierarchically across the nested haplotype network using nonparametric, exact permutation contingency tests similar to the methodology developed by Hudson et al. (1992) and implemented in GeoDis version 2.0 (Posada et al. 2000). First, a χ^2 test statistic was calculated from a simple contingency table of categorical data (rows = nested clades/haplotypes; columns = geographic locations/bacular morphotypes). Then, significance of the observed statistic was determined with an exact test against a null distribution (no association) generated by 10,000 random permutations (Edgington 1987; Roff and Bentzen 1989). These tests were used to identify the regions and/or nesting levels of the haplotype network where we find significant support for phylogeographic structure (Templeton 1995) and phenotypic associations (Templeton and Sing 1993). Tests for phylogeographic structure were conducted on both the entire dataset and the pruned data including only males of known bacular type. We did not use NCA to infer demographic history of these taxa. Although this particular application of NCA has been used extensively, the power of this approach in differentiating between various nonequilibrium population processes remains poorly understood (Knowles and Maddison 2002).

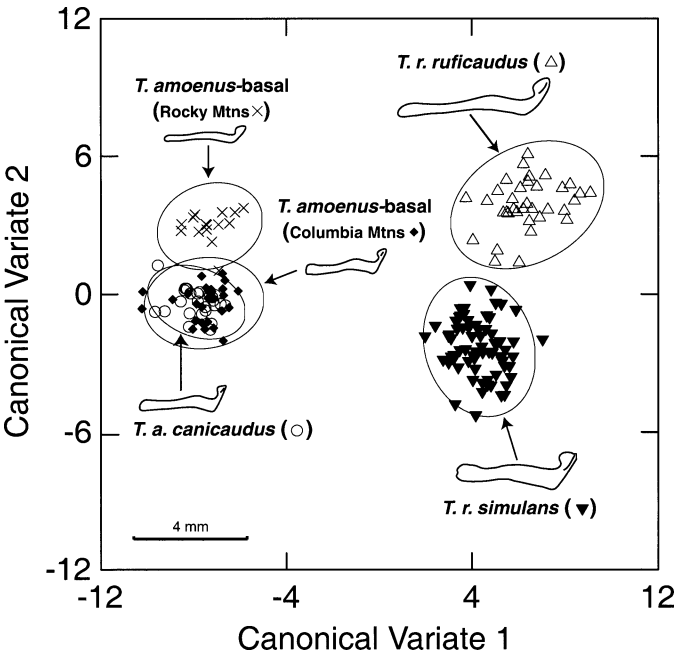

FIG. 2. Projections of bacular groupings on the first two canonical variates derived from five bacular measurements on 174 adult and subadult specimens. Symbols represent individual samples whereas ellipses indicate 95% confidence intervals about the group centroids. Bacular shapes were outlined directly from 40× right-lateral digital images.

RESULTS

Morphometric Analyses

Basic descriptive statistics for bacular measurements and ANOVA results are summarized in Table 1. The null hypothesis of equal means was strongly rejected for each of the five characters with the one-way ANOVA ($P < 0.001$). A pairwise assessment of group means with Tukey's studentized range statistic indicated that in general, excluding tip angle, nonsignificant group subsets were exclusive to *T. amoenus* and occurred between *T. amoenus*-basal CM and one of the other two *T. amoenus* groups. All comparisons between *T. a. canicaudus* and *T. amoenus*-basal RM and between *T. r. ruficaudus* and *T. r. simulans* were significantly different.

The MANOVA showed strongly significant differences among the five group centroids (Wilks' $\lambda = 0.0012$; approximate $F = 180.55$; df = 20, 548; $P < 0.0001$). The PCA (not shown) and the CVA produce very similar results suggesting four multivariate groups: *T. r. ruficaudus*, *T. r. simulans*, *T. amoenus*-basal RM, and *T. amoenus*-basal CM/*T. a. canicaudus*. The first two canonical variates (Fig. 2) accounted for 96.4% of the total dispersion (similarly, the first two principal components accounted for 90.7%). The first (83.6%) separated *T. amoenus* from *T. ruficaudus* by contrasting differences in overall bacular size, with heavy loading on tip length. The second variate contrasted bacula with long shafts and narrow bases from more robust, shorter-shafted bones and separated *T. r. ruficaudus* from *T. r. simulans* and *T. amoenus*-basal RM from *T. amoenus*-basal CM and *T. a. canicaudus*.

Identification with linear functions, combined with inspection of generalized distance statistics (D^2), supported the results of the four discrete bacular groups indicated by the CVA and PCA. *Tamias r. ruficaudus* and *T. r. simulans* specimen identification was error-free in all validation tests, with

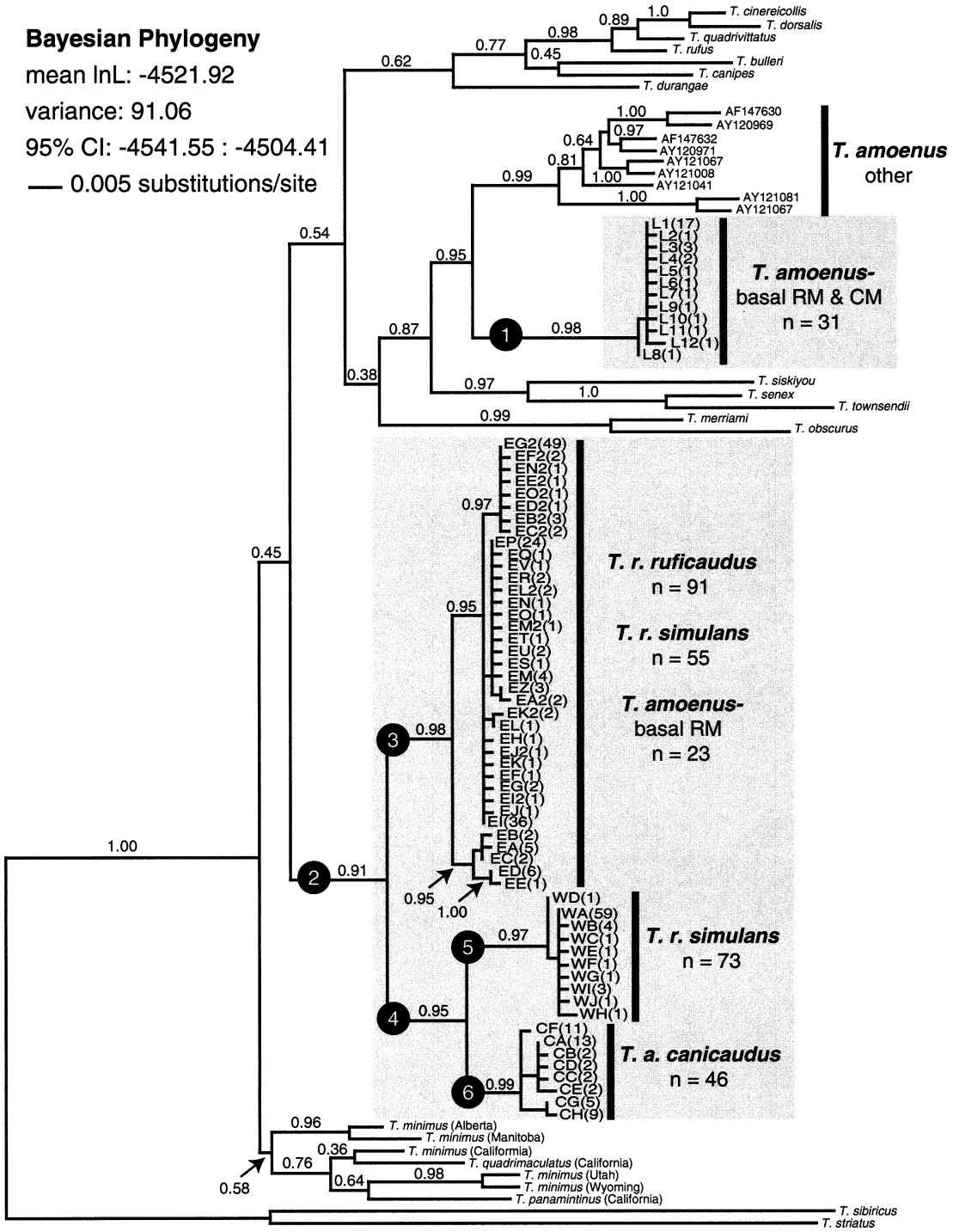

FIG. 3. One of two 50% majority-rule consensus trees from the Bayesian analysis of 97 unique sequences (701 bp of cyt *b*) estimated using the objectively chosen GTR + I + Γ (Yang 1994) model of substitution. Unique haplotypes are designated by letter/number codes with numbers in parentheses indicating the sample number for each haplotype. Circled numbers identify individual clades referenced in the text. Taxonomic composition of major clades is given based on the geographic distribution criterion depicted in Figure 1B.

unambiguous posterior probabilities of group membership ($P = 1.00$) based on D^2 statistics. Within *T. amoenus*, identification success ranged from 81% to 93% depending on the validation approach. However, within *T. amoenus*-basal RM all misidentification resulted from the allocation of one outlier (RBCM 19894), which was always classified as *T. amoenus*-basal CM (100%, $P = 0.94$) due to a much smaller tip angle (124°) than expected for this group. Other aspects of this specimen appeared consistent with characteristics of *T. amoenus*-basal RM. All other *T. amoenus*-basal RM individuals were correctly (100%) and unambiguously ($P = 1.00$) identified. Both *T. a. canicaudus* and *T. amoenus*-basal CM

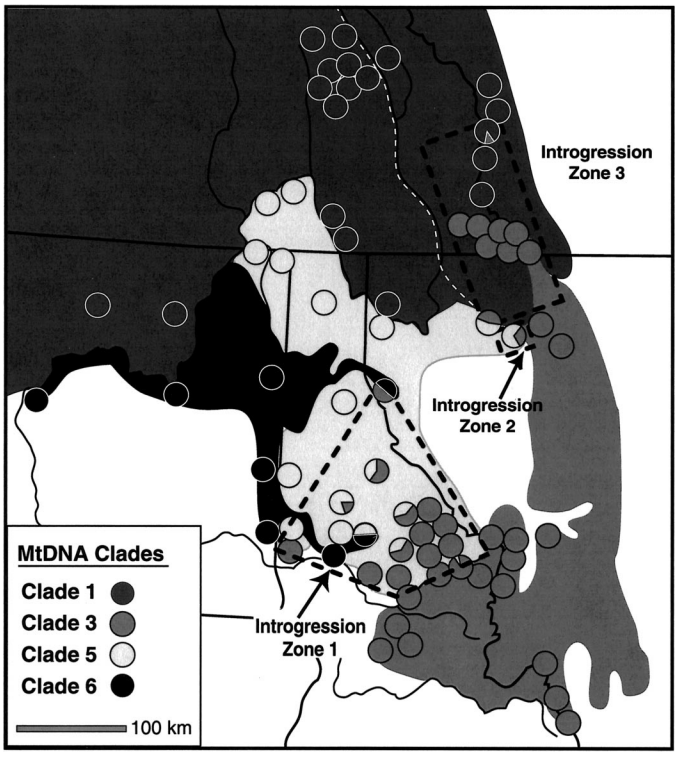

FIG. 4. The geographic distribution of major mitochondrial DNA clades (circles) overlaid on taxonomic distributions from Figure 1B (shaded background). Three geographic regions are highlighted with dotted boxes to indicate the position of the three zones of nonconcordance: (1) *Tamias ruficaudus ruficaudus*/*T. r. simulans* southern; (2) *T. r. ruficaudus*/*T. r. simulans* northern; (3) *T. r. ruficaudus*/*T. amoenus*-basal RM.

had high classification success (81–92%) despite extensive overlap in their canonical variates (Fig. 2). However, posterior probabilities of group membership indicated only 4% (1/26) of *T. a. canicaudus* and 14% (4/28) of *T. amoenus*-basal CM had significant probabilities ($P \geq 0.95$) of correct group membership. In all cases, misidentification and/or ambiguous posterior probabilities were exclusive to this pair, suggesting only very slight bacular differentiation between *T. a. canicaudus* and *T. amoenus*-basal CM. The geographic distribution of all the bacular samples fell within the taxonomic ranges specified in Figure 1B.

Phylogenetic Analyses

All sequence alignments were unambiguous, with no length polymorphisms detected. The majority rule consensus tree for one of the replicate Bayesian analyses of the 97 unique haplotypes (701 bp cyt *b*) is shown in Figure 3. In both replicates, the Markov chain appeared to reach stationarity by the 1.0×10^5 generation. Given the importance of including only samples collected at stationarity (Leaché and Reeder 2002), we used a conservative burn-in of 1.0×10^6 generations, resulting in a 4.0×10^6 generations (4.0×10^4 samples) considered for estimations of mean likelihood score, model parameters, posterior nodal probabilities, and branch lengths. Both replicates converged on very similar average log likelihood scores (ln L = −4521.92 and −4522.29), topological structure, and associated posterior nodal probabilities.

The taxonomic composition of each clade was determined using the geographic criteria depicted in Figure 1B. For example, clade 3 includes haplotypes that were sampled within the a priori geographic ranges of *T. ruficaudus* ($n = 91$), *T. simulans* ($n = 55$), and *T. amoenus*-basal RM ($n = 23$). Based on comparisons of the spatial distributions of the mtDNA clades relative to taxonomic distributions (including bacular variation), we identified three geographic zones of nonconcordance (Fig. 4). These were inferred to represent instances of asymmetric mtDNA introgression (see below). Two of these zones represented intraspecific contact between *T. r. simulans* and *T. r. ruficaudus* (introgression zone 1 and 2), while the third zone represented interspecific contact between *T. amoenus*-basal RM and *T. r. ruficaudus* (introgression zone 3). At all three contact zones, nonconcordance was characterized by the occurrence of *T. r. ruficaudus* mtDNA in populations with either *T. r. simulans* or *T. amoenus*-basal RM bacular morphotypes. The placement of all sampled *T. a. canicaudus* specimens (clade 6) within the *T. ruficaudus* clade (clade 2) and sister to *T. r. simulans* (~2.3%, uncorrected sequence divergence), was significantly supported ($P = 0.95$; clade 4, Fig. 3). Sampling of each of the major mtDNA clades in this analysis (Fig. 3) represents a subset ($n = 319$) of the total number of individuals ($n = 367$) that were typed to major mtDNA clades. Of the 48 specimens for which we typed to major mtDNA clades using a 350-bp fragment, 37 fell within clade 1, eight within clade 3, two within clade 5, and one within clade 6 (Fig. 3, Appendix). The geographic distribution of major mtDNA clades depicted in Figure 4 also summarizes this information.

The equally weighted maximum parsimony search with the dataset of 128 males of known bacular type resulted in 28 most parsimonious trees (501 steps, consistency index = 0.477, retention index = 0.897, rescaled consistency index = 0.428), all of which were consistent in overall topological structure. Figure 5 depicts one of these trees (arbitrarily chosen), with individual bacular morphotypes as determined by morphometric analyses (D^2, posterior $P \geq 0.95$; Patterson and Heaney 1987) mapped onto the terminals. The bacular morphotypes were distributed across four mtDNA clades (clades 1, 3, 5, 6; Fig. 5), all of which had high parsimony bootstrap support (98–100%). Clearly, considerable discrepancies exist between groups defined by major mtDNA clades and bacular variation, consistent with the lack of concordance

→

FIG. 5. One of 28 most parsimonious trees found with an equally weighted search of 128 males (museum voucher or accession numbers and haplotypes are indicated) of known bacular type. Bacular morphotypes were determined by multivariate analyses (D^2, posterior $P \geq 0.95$ or Patterson and Heaney 1987) are mapped onto the terminals and nodal support is given as parsimony bootstrap values (500 replicates).

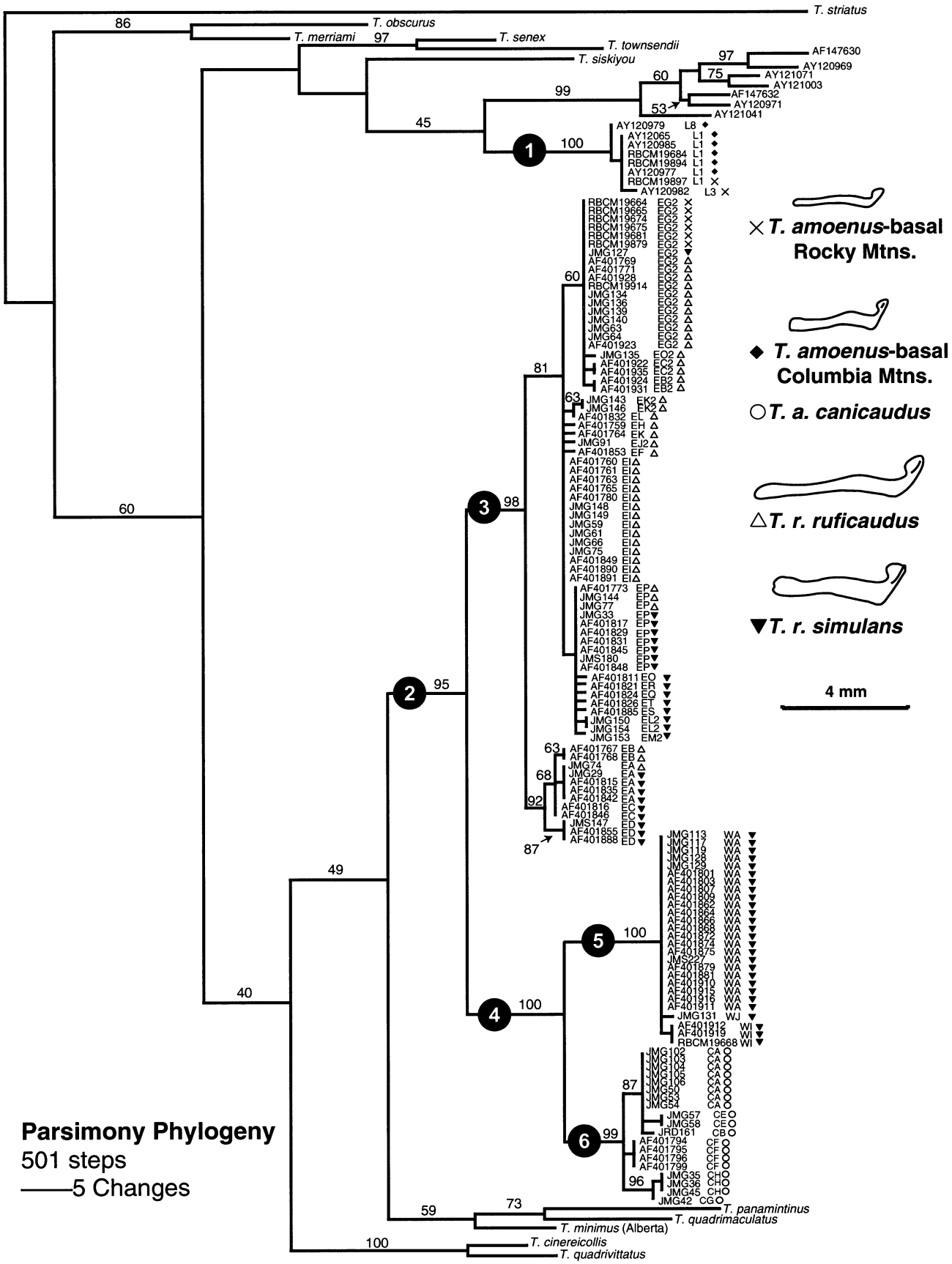
T. striatus
T. obscurus
T. merriami
T. senex
T. townsendii
T. siskiyou
AF147630
AY120969
AY121071
AY121003
AF147632
AY120971
AY121041
AY120979 L8
AY12065 L1
AY120985 L1
RBCM19684 L1
RBCM19894 L1
AY120977 L1
RBCM19897 L1
AY120982 L3
T. amoenus-basal Rocky Mtns.
T. amoenus-basal Columbia Mtns.
T. a. canicaudus
T. r. ruficaudus
T. r. simulans
4 mm
Parsimony Phylogeny
501 steps
——5 Changes
T. panamintinus
T. quadrimaculatus
T. minimus (Alberta)
T. cinereicollis
T. quadrivittatus

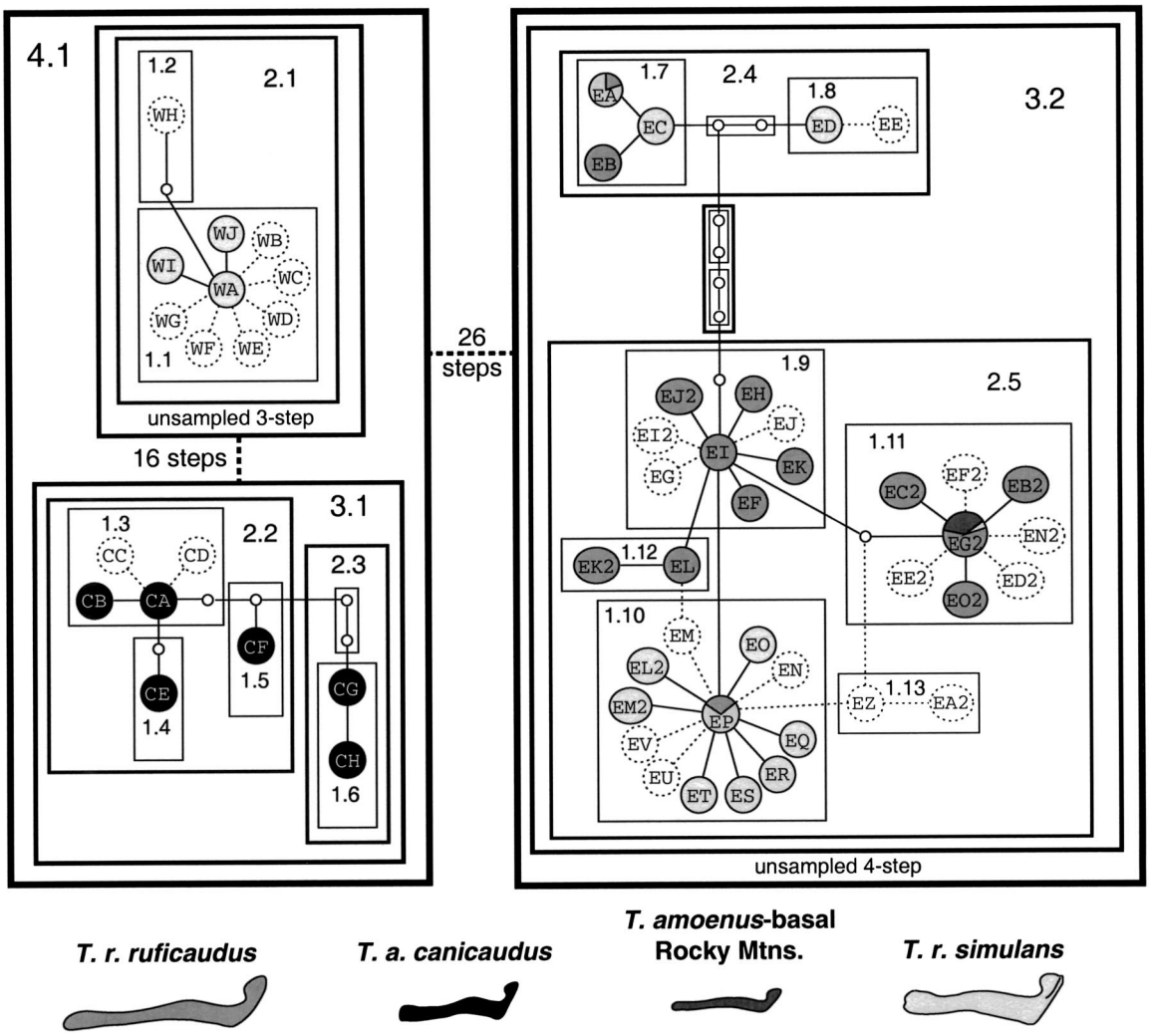

FIG. 6. Nested haplotype network showing the distribution of the four bacular morphotypes sampled within clade 2 (Figs. 3, 5). Sampled haplotypes are indicated by circled letters, unsampled haplotypes by empty circles. Haplotypes exclusive to females have dotted outlines; solid outlines indicate haplotypes found in males and/or males and females. Shading scheme indicates relative frequencies of bacular morphotypes (shown along the bottom) within a given haplotype. NCA clades 3.2, 4.1, 2.1, and 3.1 in this figure correspond to clades 3, 4, 5, and 6, respectively, from Figures 3 and 5.

found in the geographic overlay (Fig. 4). In particular, we sampled three of the four observed bacular morphotypes within clade three. It should be noted that an additional 26 specimens with *T. amoenus*-basal RM ($n = 8$) and CM ($n = 18$) bacula were typed to mtDNA clade one (Fig. 5) using the 350-bp alignment.

Nested Clade Analyses

For 701 bp, haplotypes connected by ≤11 substitutions fall within the 95% plausibility set ($P \geq 0.9538$); this criterion subdivided the data into three networks (NCA clades 2.1, 3.1, 3.2; Fig. 6). These partitions corresponded exactly with the *T. r. simulans*, *T. a. canicaudus*, and *T. r. ruficaudus* clades identified with phylogenetic analyses (clades 5, 6, and 3; Figs. 3, 5). Interconnections between networks estimated with PAUP* indicated that the *T. a. canicaudus* NCA clade (3.1) was connected by a minimum of 16 observed substitutions to the *T. r. simulans* NCA clade (2.1) and a minimum of 26 substitutions to the *T. r. ruficaudus* NCA clade (3.2). Using the formula developed by Templeton et al. (1992) and executed with ParsProb version 1.1 (Posada 2000), the probability of these connections were $P = 0.9066$ and $P = 0.7743$. However, the separate Bayesian phylogenetic analysis united *T. a. canicaudus* (NCA clade 3.1) and *T. r. simulans* (NCA clade 2.1) with a posterior probability of $P = 1.00$. This provided a more robust statistical justification of the nesting of NCA clade 4.1 (Fig. 6) and is consistent with other phylogenetic analyses (clade 4, Fig. 3).

Categorical testing of the association between haplotype structure and both geographic localities and bacular types is given in Table 2. In general, we found considerable phylogeographic structure across the network that was consistent when considering either the entire dataset or only males of known bacular type. Bacular morphotypes were also highly structured across the NCA network, including a strongly significant nonrandom distribution within NCA clades 3.2 ($P =$

TABLE 2. Nested contingency analysis of geographic and morphometric categorical associations. Significance (shown in bold) of the observed χ^2-statistic was determined with an exact test against a null distribution (no association) generated by 10,000 random permutations. Geographic analyses were conducted on both the entire dataset ($n = 288$) and the subset of males of known bacular type ($n = 120$). Dashes indicate NCA clades that are either nonvariable or unsampled.

NCA clade	Geographic localities: All samples χ^2 (P)	Geographic localities: Males only χ^2 (P)	Bacula χ^2 (P)
1.1	**256.37 (0.0008)**	30.52 (0.1413)	—
1.3	**27.30 (0.0438)**	9.00 (0.1096)	—
1.6	4.32 (0.0835)	1.33 (1.00)	—
1.7	14.85 (0.3586)	14.85 (0.4695)	5.40 (0.1640)
1.8	7.00 (0.7136)	—	—
1.9	110.16 (0.3345)	27.42 (0.6482)	—
1.10	227.35 (0.1075)	79.20 (0.8368)	2.88 (1.00)
1.11	139.25 (0.0789)	11.12 (0.9846)	3.16 (0.7136)
1.12	3.00 (0.3348)	3.00 (0.3335)	—
1.13	2.22 (0.4074)	—	—
2.1	36.49 (0.0949)	30.52 (0.1413)	—
2.2	**64.00 (<0.0001)**	**30.00 (<0.0001)**	—
2.4	9.23 (0.4745)	8.44 (0.7759)	4.00 (0.1755)
2.5	**347.13 (<0.0001)**	**109.87 (0.0014)**	**53.46 (<0.0001)**
3.1	**38.27 (<0.0001)**	**19.00 (0.0015)**	—
3.2	**81.31 (0.0004)**	**45.17 (0.0048)**	**11.07 (0.0070)**
4.1	**117.18 (<0.0001)**	**46.00 (<0.0001)**	**46.00 (<0.0001)**
Total	**238.58 (<0.0001)**	**116.37 (<0.0001)**	**65.09 (<0.0001)**

0.0128) and 2.5 ($P < 0.0001$; Table 2, Fig. 5), where the majority of the nonconcordance was observed (Figs. 3, 5, 6). When considering these data in a geographic context, we found the following general patterns consistent with asymmetric introgressive hybridization. Instances of nonconcordance were geographically localized to regions of current taxonomic and morphological contact (Fig. 4). In three of these regions (Fig. 4), we found identical high-frequency interior haplotypes shared between the nonconcordant localities and adjacent parental populations. Haplotypes found only in nonconcordant populations tended to be in low-frequency and geographically restricted one-step mutational variants of the higher-frequency shared haplotypes.

As observed by Good and Sullivan (2001), the geographic contact of bacular morphotypes in introgression zone 1 corresponded precisely to either side of the Lochsa River (a tributary in the Clearwater River drainage), whereas mitochondrial variation within this drainage was almost completely characterized by haplotypes of NCA clade 3.2 (clade 3; Figs. 3, 5). The geographic limits of *T. r. ruficaudus* bacula in this area coincided exactly with the northern distribution of NCA clades 1.9 and 1.12. The frequency of *T. r. simulans* haplotypes (NCA clade 2.1) within this region was extremely low. Introgression between *T. r. ruficaudus* and *T. r. simulans* in northwestern Montana (introgression zone 2) was more geographically restricted. Here we found evidence for introgression at a single locality (locality 68, Fig. 1) of mixed *T. r. simulans* (NCA clade 2.1) and *T. r. ruficaudus* (NCA clade 1.11) haplotypes with *T. r. simulans* morphology. Approximately 30 km northeast of this location (locality 70, Fig. 1) all individuals sampled were parental *T. r. ruficaudus*, suggesting possible morphological contact in the intervening geography. The introgression between *T. r. ruficaudus* and *T. amoenus*-basal RM occurred north and west of introgression zone 2 along a broadly defined ecological transition. At seven localities (Fig. 1; localities 17, 18, 19, 22, 23, 24, 69) specimens of *T. amoenus*-basal RM ($n = 22$) possessed haplotypes found only within NCA clade 1.11 (part of *T. r. ruficaudus* clade 3; Figs. 3, 5). These included females also identified by genital bone morphology (os clitoris; D. W. Nagorsen, unpubl. data), suggesting complete *T. r. ruficaudus* mtDNA fixation within this region. In addition, one specimen of *T. amoenus*-basal RM with a NCA clade 1.11 haplotype (EG2) was sampled at locality 27.

DISCUSSION

Phylogeographic Analyses and Introgressive Hybridization

Differentiating between introgression and incomplete sorting of ancestral polymorphisms is essential in resolving nonconcordance among character sets in closely related taxa (Avise and Ball 1990). Establishing phylogeographic patterns provides an objective assessment of this issue, because each of these processes should generate a specific spatial pattern (Goodman et al. 1999). Recent hybridization should result in introgressed alleles that are more common near current contact zones, whereas ancestral polymorphisms should be diffused at approximately uniform frequency (Barbujani et al. 1994). The spatial structure of nonconcordance contained within NCA clade 3.2 and the sharing of identical haplotypes across contact zones suggests that incomplete sorting can be ruled out as a reasonable explanation for nonconcordance at introgression zones 1–3 (Figs. 4, 6; Table 2).

Given the patterns of asymmetric introgression between *T. amoenus* and *T. ruficaudus*, the phylogenetic placement of *T. a. canicaudus* mtDNA (clade 6; Figs. 3, 5) most likely reflects fixation following an ancient mtDNA introgression event between ancestral populations of *T. amoenus* and *T. r. simulans*. Under this scenario, it would appear that mtDNA introgression among these contiguously distributed taxa was a nonrecurrent event, given the lack of available evidence for recent mtDNA haplotype exchange. However, at least two vi-

able alternatives to an ancient introgression interpretation exist.

First, the observed mtDNA gene tree may represent an accurate estimation of species relationships and the taxon identified as *T. a. canicaudus* may be a distinct evolutionary lineage within *T. ruficaudus*. This would require fairly rapid bacular and ecological convergence of this taxon with *T. amoenus* given the relatively short branch separating *T. a. canicaudus* from *T. r. simulans*. Although some interspecific convergence of pelage coloration and cranial morphology in response to environmental selection may have occurred within the radiation of western chipmunks (Sutton and Patterson 2000), such extreme convergence in bacular form among geographically juxtaposed taxa (i.e., *T. a. canicaudus* and *T. amoenus*-basal CM) has never been demonstrated. In fact, in the Columbia Mountains, *T. amoenus*-basal CM and *T. r. simulans* exhibit convergence in pelage and cranial traits but maintain their strongly divergent bacular forms (D. W. Nagorsen, unpubl. data). Support for the convergence hypothesis would require additional phylogenetic data from unlinked nuclear loci consistent with the evolutionary relationships suggested by mtDNA.

Alternatively, the observed mtDNA gene tree may differ from the species tree due to incomplete sorting of ancestral polymorphisms (Neigel and Avise 1986; Hudson 1992). This would seem improbable given *T. ruficaudus* and *T. amoenus* are divergent nonsister taxa (Fig. 3; Piaggio and Spicer 2001). Furthermore, the haploid and uniparental inheritance of mtDNA should result in a small effective population size (Birky et al. 1989) and a relatively shallow coalescence time in this marker (Moore 1995) for chipmunks. This would reduce the plausibility of incomplete lineage sorting as an explanation for this pattern.

Once the occurrence of introgressive hybridization has been established, the regional biogeographic history and the evolutionary relationships among haplotypes are useful in evaluating the relative age of independent, temporally layered introgression events. Inferred introgression between *T. a. canicaudus* and *T. r. simulans* clearly represents an older and nonrecurrent event. Conversely, all three introgression zones (Fig. 4) involve sharing of identical haplotypes between the hybrid and parental populations (haplotype EP in introgression zone 1 and haplotype EG2 in introgression zones 2 and 3), suggesting that introgression between these populations are recent and potentially ongoing evolutionary events. The geographic distribution and haplotype diversity and structure (including numerous rare haplotypes unique to the introgressed population) within zone 1 indicate that hybridization within this region most likely predates hybridization at zones 2 and 3. This observation is consistent with the geological and climatic history of the region. Several authors have postulated that thermal retention within the Clearwater Drainage (i.e., introgression zone 1) may have enabled regional biota to persist in this area at least during the last major Pleistocene glaciation (e.g., Daubenmire 1975; Johnson 1988), and perhaps throughout the Pleistocene (Nielson et al. 2001). Regional refugia and/or early postglacial recolonization and secondary contact of *T. r. ruficaudus* and *T. r. simulans* populations in the proximity of zone 1 could be associated with the relative antiquity of introgression in this area. Conversely, re-establishment of suitable habitat within the proximity of zones 2 and 3 could not have occurred prior to glacial retreat ($<$12,000 years ago, Clague 1981).

In general, these phylogeographic and morphometric data provide an initial identification of hybridization among poorly resolved taxa that may be used to guide future data collection specifically focused on fine-scale analysis of the identified hybrid zones. The multiple instances of extensive introgression of *T. ruficaudus* mtDNA across taxonomic boundaries may reflect the action of positive selection on the introgressed mitochondrial genome or hitchhiking associated with positively selected nuclear genes (Kilpatrick and Rand 1995). Likewise, the patterns we find may be associated with neutral diffusion and hybrid zone movement (Arntzen and Wallis 1991) and/or historical founder effects (Gyllensten and Wilson 1987). Regardless, a thorough discussion of these scenarios awaits data addressing the nature of clinal variation of multiple unlinked nuclear loci across each zone.

Evolutionary Implications of Asymmetric Introgression

Asymmetric introgression of animal mtDNA is not uncommon (Jaarola et al. 1997; Ruedi et al. 1997; Ross and Harrison 2002) and can arise through differential gene flow associated with asymmetry in both pre- and postzygotic isolation (Wirtz 1999). In general, hybrid females backcrossing to parental populations will mediate the movement of maternally inherited mtDNA across hybrid zones in mammalian systems. At a minimum, the patterns of introgression inferred here must have been generated by reproduction between *T. r. ruficaudus* females and *T. r. simulans*/*T. amoenus* males. We have found no evidence for reciprocal crosses. This pattern may be due to prezygotic isolation or reduced fitness of offspring from these reciprocal crosses. Sexual isolation is often directional between hybridizing species (Coyne and Orr 1998), although the evolutionary basis for this pattern remains controversial (Kaneshiro 1980; Arnold et al. 1996).

One intriguing possibility is the potential role of reproductive barriers associated with variation in genital morphology toward promoting sexual isolation. It has been argued that interspecific differentiation in animal phallic morphology results from direct selection for reproductive isolating mechanisms among incipient species (Patterson and Thaeler 1982; Sota and Kubota 1998). In general, the evolutionary processes driving differentiation of animal genitalia remains controversial and several viable alternatives to the lock-and-key interpretation exist (for reviews, see Eberhard 1985; Arnqvist 1997). In *Tamias*, a lock-and-key explanation of bacular divergence is based on the protrusion of the baculum from the glans during copulation (Adams and Sutton 1968) and subsequent potential to perform a species-specific reproductive function (Patterson and Thaeler 1982). The extent to which bacular differentiation in *Tamias* results in, or is predictive of, reproductive isolation has never been directly addressed. Directionality of interspecific crosses inferred here may be associated with overall bacular size, where females from a parental mating system with large bacula (*T. ruficaudus*) are crossing with males with substantially smaller bacula (*T. amoenus*). This general pattern holds for the intraspecific hybridization between *T. r. ruficaudus* (females) and *T. r.*

simulans (males), albeit size differences here are much less pronounced. Nevertheless, the extent to which gross bacular morphology plays a mechanistic role in reproductive isolation in chipmunks remains speculative.

Introgressive Hybridization and Systematics

The frequency and evolutionary role of widespread character introgression in animals remains unclear (Dowling and Secor 1997). We have demonstrated multiple independent examples of extensive asymmetric introgression among taxa from divergent mtDNA lineages with distinct bacular morphology. These events represent the first indication of hybridization within *Tamias* and demonstrate that the assumption of complete reproductive isolation between chipmunk species with distinct bacular morphology can be violated. It has been shown elsewhere that even rare hybridization can have a pronounced effect on the genetic composition of codistributed taxa (Goodman et al. 1999). Based on our data, it is clear that potential hybridization must be considered when assessing the systematic relationships within *Tamias* regardless of persistent morphological and/or ecological distinctness.

MtDNA gene trees have provided a powerful tool in the examination of intra- and interspecific phylogeography (Avise 2000), as well as a tractable means of species delimitation (Leaché and Reeder 2002; Wiens and Penkrot 2002). Indeed, phylogenetic studies within and among closely related species have come to be dominated by mtDNA data. However, the apparent susceptibility of mtDNA to introgressive hybridization and reticulate evolution poses some interesting challenges to its utility in evaluations of species limits (Ruedi et al. 1997). In general, the use of mtDNA genealogies, in conjunction with other data, to identify specific evolutionary lineages has proven very powerful (e.g., Matocq 2002). However, our results suggest caution when equating taxa with nonexclusive mtDNA lineages as conspecific. The semipermeable nature of many hybrid zones has repeatedly been shown to result in mtDNA introgression under a variety of population histories (Harrison 1989; Dowling and Hoeh 1991), suggesting mtDNA introgression is a poor indicator of extensive nuclear gene flow.

Acknowledgments

We thank M. Fraker, D. Good, J. Good, P. Good, J. Harper, S. Poler, D. Sullivan, and the 1997–2001 University of Idaho Mammalogy classes for their assistance with field collection. We thank J. Kenagy and B. Arbogast (Burke Museum of Natural History and Culture), N. Panter (Royal British Columbia Museum), B. Patterson (Field Museum of Natural History), and K. Pullen (Connor Museum of Natural History) for additional samples. We also thank S. Brunsfeld, J. Byers, B. Carstens, K. Crandall, P. Joyce, W. Maddison, J. Patton, B. Payseur, J. Wiens, and the BYU phylogeography reading group for helpful discussions regarding the methodology and conceptual development of this manuscript. This research was supported by a seed grant from the University of Idaho Research Foundation, the EPSCoR program (NSF cooperative agreement number EPS-9720634), and the Initiative for Bioinformatics and Evolutionary Studies (IBEST) at the University of Idaho (by NCRR grant 1P20RR016454-01; NIH NCRR grant 1P20RR016448-01; NSF grant EPS-809935). Some of the equipment used for this study was provided by DHHS/NIH RR11833 to the University of Idaho, Department of Biological Sciences, and V. Eroschenko.

Literature Cited

Adams, D. R., and D. A. Sutton. 1968. A description of the baculum and the os clitoris of *Eutamias townsendii ochrogenys*. J. Mammal. 49:764–768.

Anderson, E. 1949. Introgressive hybridization. Wiley, New York.

Arnold, S. J., P. A. Verrel, and S. G. Tilley. 1996. The evolution of asymmetry in sexual isolation: a model and a test case. Evolution 50:1024–1033.

Arnqvist, G. 1997. The evolution of animal genitalia: distinguishing between hypotheses by single species studies. Biol. J. Linn. Soc. 60:365–379.

Arntzen, J. W., and G. P. Wallis. 1991. Restricted gene flow in a moving hybrid zone of the newts *Triturus cristatus* and *Triturus marmoratus* in western France. Evolution 45:805–826.

Avise, J. C. 2000. Phylogeography: the history and formation of species. Harvard Univ. Press, Cambridge, MA.

Avise, J. C., and R. M. J. Ball. 1990. Principles of genealogical concordance in species concepts and biological taxonomy. Pp. 45–67 *in* D. Futuyma and J. Antonovics, eds. Oxford surveys in evolutionary biology. Oxford Univ. Press, New York.

Barbujani, G., A. Pilastro, S. Dedomenico, and C. Renfrew. 1994. Genetic variation in North Africa and Eurasia-Neolithic demic diffusion vs. Paleolithic colonization. Am. J. Phys. Anthropol. 95:137–154.

Barton, N. H. 2001. The role of hybridization in evolution. Mol. Ecol. 10:551–568.

Barton, N. H., and G. M. Hewitt. 1985. Analysis of hybrid zones. Annu. Rev. Ecol. Syst. 16:113–148.

Beg, M. A., and R. S. Hoffman. 1977. Age determination and variation in the red-tailed chipmunk, *Eutamias ruficaudus*. Murrelet 58:26–36.

Best, T. L. 1993. *Tamias ruficaudus*. Mammal. Species 452:1–7.

Bibb, M. J., R. A. Van Etten, C. T. Wright, M. W. Walberg, and D. A. Clayton. 1981. Sequence and gene organization of mouse mitochondrial DNA. Cell 26:167–180.

Birky, C. W., Jr., P. Fuerst, and T. Maruyama. 1989. Organelle gene diversity under migration, mutation and drift: equilibrium expectations, approach to equilibrium, effects of heteroplasmic cells, and comparisons to nuclear genes. Genetics 121:613–627.

Brown, J. H. 1971. Mechanisms of competitive exclusion between two species of chipmunks. Ecology 52:305–311.

Brumfield, R. T., R. W. Jernigan, D. B. McDonald, and M. J. Braun. 2001. Evolutionary implications of divergent clines in an avian (*Manacus*: Aves) hybrid zone. Evolution 55:2070–2087.

Callahan, J. R. 1977. Diagnosis of *Eutamias obscurus* (Rodentia: Sciutidae). J. Mammal. 58:188–201.

Castelloe, J., and A. R. Templeton. 1994. Root probabilities for intraspecific gene trees under neutral coalescent theory. Mol. Phylogenet. Evol. 3:102–113.

Chappell, M. A. 1978. Behavioral factors in the altitudinal zonation of chipmunks (*Eutamias*). Ecology 59:565–579.

Clague, J. J. 1981. Late Quaternary geology and geochronology of British Columbia. 2. Summary and discussion of radiocarbon-dated Quaternary history. Pp. 41. Paper 80–35. Geological Survey of Canada, Ottawa, Canada.

Clement, M., D. Posada, and K. A. Crandall. 2000. TCS: a computer program to estimate gene genealogies. Mol. Ecol. 9:1657–1659.

Coyne, J. A., and H. A. Orr. 1998. The evolutionary genetics of speciation. Philos. Trans. R. Soc. Lond. B Biol. Sci. 353: 287–305.

Crandall, K. A. 1996. Multiple interspecies transmissions of human and simian T-cell leukemia/lymphoma virus type I sequences. Mol. Biol. Evol. 13:115–131.

Crandall, K. A., and A. R. Templeton. 1993. Empirical tests of

some predictions from coalescent theory with applications to intraspecific phylogeny reconstruction. Genetics 134:959–969.
Daubenmire, R. 1975. Floristic plant geography of eastern Washington and northern Idaho. J. Biogeogr. 2:1–18.
Demboski, J. R., and J. Sullivan. 2003. Extensive mtDNA variation within the yellow-pine chipmunk, *Tamias amoenus* (Rodentia: Sciuridae), and phylogeographic inferences for northwest North America. Mol. Phylogenet. Evol. 26:389–408
Dobzhansky, T. 1950. Mendelian populations and their evolution. Am. Nat. 84:401–418.
Dowling, T. E., and W. R. Hoeh. 1991. The extent of introgression outside the contact zone between *Notropis cornutus* and *Notropis chrysocephalus* (Teleostei: Cyprinidae). Evolution 45:944–956.
Dowling, T. E., and C. L. Secor. 1997. The role of hybridization and introgression in the diversification of animals. Annu. Rev. Ecol. Syst. 28:593–619.
Eberhard, W. G. 1985. Sexual selection and the evolution of animal genitalia. Harvard Univ. Press, Cambridge, MA.
Edgington, E. S. 1987. Randomization tests. Marcel, New York.
Good, J. M., and J. Sullivan. 2001. Phylogeography of the red-tailed chipmunk (*Tamias ruficaudus*), a northern Rocky Mountain endemic. Mol. Ecol. 10:2683–2695.
Goodman, S. J., N. H. Barton, G. Swanson, K. Abernethy, and J. M. Pemberton. 1999. Introgression through rare hybridization: a genetic study of a hybrid zone between red and sika deer (genus *Cervus*) in Argyll, Scotland. Genetics 152:355–371.
Gustincich, S., G. Manfioletti, C. Schneider, and P. Carninci. 1991. A fast method for high-quality genomic DNA extraction from whole human blood. Biotechniques 11:298–302.
Gyllensten, U., and A. C. Wilson. 1987. Interspecific mitochondrial DNA transfer and the colonisation of Scandinavia by mice. Genet. Res. 49:25–29.
Haldane, J. B. S. 1948. The theory of a cline. J. Genet. 48:277–284.
Hall, E. R. 1981. The mammals of North America. Wiley, New York.
Hare, M. P., F. Cipriano, and S. R. Palumbi. 2002. Genetic evidence on the demography of speciation in allopatric dolphin species. Evolution 56:804–816.
Harrison, R. G. 1989. Animal mitochondrial DNA as a genetic marker in population and evolutionary biology. Trends Ecol. Evol. 4:6–11.
Harrison, R. G., and S. M. Bogdanowicz. 1997. Patterns of variation and linkage disequilibrium in a field cricket hybrid zone. Evolution 51:493–505.
Hewitt, G. M. 1989. The subdivision of species by hybrid zones. Pp. 85–110 *in* D. Otte and J. A. Endler, eds. Speciation and its consequences. Sinauer, Sunderland, MA.
Hoffmann, R. S., and D. L. Pattie. 1968. A guide to Montana mammals: identification, habitat, distribution and abundance. Univ. of Montana, Missoula.
Howell, A. H. 1929. Revision of the American chipmunks (genera *Tamias* and *Eutamias*). N. Am. Fauna 52:1–157.
Hudson, R. R. 1992. Gene trees, species trees and the segregation of ancestral alleles. Genetics 131:509–512.
Hudson, R. R., D. D. Boos, and N. L. Kaplan. 1992. A statistical test for detecting geographic subdivision. Mol. Biol. Evol. 9: 138–151.
Huelsenbeck, J. P., and N. S. Imennov. 2002. Geographic origin of human mitochondrial DNA: accommodating phylogenetic uncertainty and model comparison. Syst. Biol. 51:155–165.
Huelsenbeck, J. P., and F. Ronquist. 2001. MRBAYES: Bayesian inference of phylogenetic trees. Bioinformatics 17:754–755.
Jaarola, M., H. Tegelström, and K. Fredga. 1997. A contact zone with noncoincident clines for sex-specific markers in the field vole (*Microtus agrestis*). Evolution 51:241–249.
Johnson, D. L. 1943. Systematic review of the chipmunks (genus *Eutamias*) of California. Univ. Calif. Publ. Zool. 48:63–148.
Johnson, P. J. 1988. Larval taxonomy, and biogeography of the genera of North America Byrridae (Insecta: Coleoptera). M.S. thesis, University of Idaho, Moscow, ID.
Kaneshiro, K. V. 1980. Sexual isolation, speciation, and the direction of evolution. Evolution 34:437–444.
Kilpatrick, S. T., and D. M. Rand. 1995. Conditional hitchhiking of mitochondrial DNA: frequency shifts of *Drosophila melanogaster* mtDNA variants depend on nuclear genetic background. Genetics 141:1113–1124.
Knowles, L. L., and W. P. Maddison. 2002. Statistical phylogeography. Mol. Ecol. 11:2623–2635.
Kocher, T. D., W. K. Thomas, A. Meyer, S. V. Edwards, S. Pääbo, F. X. Villablanca, and A. C. Wilson. 1989. Dynamics of mitochondrial DNA evolution in animals: amplification and sequencing with conserved primers. Proc. Natl. Acad. Sci. USA 86: 6196–6200.
Lance, R. F., M. L. Kennedy, and P. L. Leberg. 2000. Classification bias in discriminant function analyses used to evaluate putatively different taxa. J. Mammal. 81:245–249.
Leaché, A. D., and T. W. Reeder. 2002. Molecular systematics of the eastern fence lizard (*Sceloporus undulatus*): a comparison of parsimony, likelihood, and Bayesian approaches. Syst. Biol. 51: 44–68.
Mahalanobis, P. C. 1936. On the generalized distance in statistics. Proc. Natl. Inst. Sci. India 2:49–55.
Matocq, M. D. 2002. Morphological and molecular analysis of a contact zone in the *Neotoma fuscipes* species complex. J. Mammal. 83:866–883.
Matos, J. A., and B. A. Schaal. 2000. Chloroplast evolution in the *Pinus montezumae* complex: a coalescent approach to hybridization. Evolution 54:1218–1233.
Mayr, E. 1963. Animal species and evolution. Harvard Univ. Press, Cambridge, MA.
Merriam, C. H. 1903. Eight new mammals from the United States. Proc. Biol. Soc. Wash. 16:73–78.
Moore, W. S. 1995. Inferring phylogenies from mtDNA variation: mitochondrial-gene trees versus nuclear-gene trees. Evolution 49:718–726.
Neigel, J. E., and J. C. Avise. 1986. Phylogenetic relationships of mitochondrial DNA under various demographic models of speciation. Pp. 515–534 *in* E. Nevo and S. Karlin, eds. Evolutionary processes and theory. Academic Press, New York.
Nielson, M., K. Lohman, and J. Sullivan. 2001. Phylogeography of the tailed frog (*Ascaphus truei*): implications for the biogeography of the Pacific Northwest. Evolution 55:147–160.
Orthmeyer, D. L., J. Y. Takekawa, C. R. Ely, M. L. Wege, and W. E. Newton. 1995. Morphological differences in Pacific Coast populations of greater white-fronted geese. Condor 97:123–132.
Patterson, B. D. 1982. Pleistocene vicariance, montane islands, and the evolutionary divergence of some chipmunks (genus *Eutamias*). J. Mammal. 63:387–398.
Patterson, B. D., and L. R. Heaney. 1987. Preliminary analysis of geographic variation in red-tailed chipmunks (*Eutamias ruficaudus*). J. Mammal. 68:782–791.
Patterson, B. D., and C. S. J. Thaeler. 1982. The mammalian baculum: hypotheses on the nature of bacular variability. J. Mammal. 63:1–15.
Piaggio, A. J., and G. S. Spicer. 2001. Molecular phylogeny of the chipmunks inferred from mitochondrial cytochrome *b* and cytochrome oxidase II gene sequences. Mol. Phylogenet. Evol. 20: 335–350.
Posada, D. 1999. COLLAPSE. Ver. 1.1. Available via http://zoology.byu.edu/crandall_lab/programs.htm
———. 2000. ParsProb. Ver. 1.1. Available via http://zoology.byu.edu/crandall_lab/programs.htm
Posada, D., and K. A. Crandall. 2001. Intraspecific gene genealogies: trees grafting into networks. Trends Ecol. Evol. 16:37–45.
Posada, D., K. A. Crandall, and A. R. Templeton. 2000. GeoDis: a program for the cladistic nested analysis of the geographical distribution of genetic haplotypes. Mol. Ecol. 9:487–488.
Reyment, R. A., R. E. Blackith, and N. A. Campbell. 1984. Multivariate morphometrics. Academic Press, Orlando, FL.
Rieseberg, L. H., J. Whitton, and K. Gardner. 1999. Hybrid zones and the genetic architecture of a barrier to gene flow between two sunflower species. Genetics 152:713–727.
Roff, D. A., and P. Bentzen. 1989. The statistical analysis of mitochondrial DNA polymorphism: chi-square and the problem of small samples. Mol. Biol. Evol. 6:539–545.
Ross, C. L., and R. G. Harrison. 2002. A fine-scale analysis of the

mosaic hybrid zone between *Gryllus firmus* and *Gryllus pennsylvanicus*. Evolution 56:2296–2312.
Ruedi, M., M. F. Smith, and J. L. Patton. 1997. Phylogenetic evidence of mitochondrial DNA introgression among pocket gophers in New Mexico (family Geomyidae). Mol. Ecol. 6: 453–462.
Sota, T., and K. Kubota. 1998. Genital lock-and-key as a selective agent against hybridization. Evolution 52:1507–1513.
Sota, T., R. Ishikawa, M. Ujiie, F. Kusumoto, and A. P. Vogler. 2001. Extensive trans-species mitochondrial polymorphisms in the carabid beetles *Carabus* subgenus *Ohmopterus* caused by repeated introgressive hybridization. Mol. Ecol. 10:2833–2847.
Spencer, M. A., and G. S. Spencer. 1994. MacMorph: morphometric data acquisition software. Ver. 2.1. Available via http://carbon.cudenver.edu/~mspencer/MacMorphPage.html
Sullivan, J., J. Markert, and C. W. Kilpatrick. 1997. Phylogeography and molecular systematics of the *Peromyscus aztecus* species group (Rodentia: Muridae) inferred using parsimony and likelihood. Syst. Biol. 46:426–440.
Sullivan, J., E. Arellano, and D. S. Rogers. 2000. Comparative phylogeography of Mesoamerican highland rodents: concerted versus independent responses to past climatic fluctuations. Am. Nat. 155:755–768.
Sutton, D. A. 1992. *Tamias amoenus*. Mammal. Species 390:1–8.
Sutton, D. A., and C. F. Nadler. 1974. Systematics revision of three Townsend chipmunks (*Eutamias townsendii*). Southwest. Nat. 19:199–212.
Sutton, D. A., and B. D. Patterson. 2000. Geographic variation of the western chipmunks *Tamias senex* and *T. siskiyou*, with two new subspecies from California. J. Mammal. 81:299–316.
Swofford, D. L. 2000. PAUP*: phylogenetic analysis using parsimony (* and other methods). Sinauer, Sunderland, MA.
Templeton, A. R. 1994. The role of molecular genetics in speciation studies. Pp. 455–477 *in* B. Schierwater, B. Streit, G. P. Wagner, and R. DeSalle, eds. Molecular ecology and evolution: approaches and applications. Birkhäuser, Basel.
———. 1995. A cladistic analysis of phenotypic associations with haplotypes inferred from restriction endonuclease mapping or DNA sequencing. V. Analysis of case/control sampling designs: Alzheimer's disease and the Apoprotein E locus. Genetics 140: 403–409.
———. 2001. Using phylogeographic analyses of gene trees to test species status and process. Mol. Ecol. 10:779–791.
Templeton, A. R., and C. F. Sing. 1993. A cladistic analysis of phenotypic associations with haplotypes inferred from restriction endonuclease mapping. IV. Nested analyses with cladogram uncertainty and recombination. Genetics 134:659–669.
Templeton, A. R., E. Boerwinkle, and C. F. Sing. 1987. A cladistic analysis of phenotypic associations with haplotypes inferred from restriction endonuclease mapping. I. Basic theory and an analysis of alcohol dehydrogenase activity in *Drosophila*. Genetics 117:343–351.
Templeton, A. R., K. A. Crandall, and C. F. Sing. 1992. A cladistic analysis of phenotypic associations with haplotypes inferred from restriction endonuclease mapping and DNA sequence data. III. Cladogram estimation. Genetics 132:619–633.
Templeton, A. R., E. Routman, and C. A. Phillips. 1995. Separating population structure from population history: a cladistic analysis of the geographical distribution of mitochondrial DNA haplotypes in the tiger salamander, *Ambystoma tigrinum*. Genetics 140: 767–782.
White, J. A. 1953. The baculum in the chipmunks of western North America. Univ. Kans. Publ. Mus. Nat. Hist. 5:611–631.
Wiens, J. J., and T. A. Penkrot. 2002. Delimiting species using DNA and morphological variation and discordant species limits in spiny lizards (*Sceloporus*). Syst. Biol. 51:69–91.
Wirtz, P. 1999. Mother species-father species: unidirectional hybridization in animals with female choice. Anim. Behav. 58: 1–12.
Yang, Z. 1994. Maximum likelihood phylogenetic estimation from DNA sequences with variable rates over sites: approximate methods. J. Mol. Evol. 39:306–314.
Yang, Z., N. Goldman, and A. Friday. 1995. Maximum likelihood trees from DNA sequences: a peculiar statistical estimation problem. Syst. Biol. 44:384–399.

Corresponding Editor: J. Wiens

Appendix

Sampling localities and specimen information. Locality numbers correspond to designations in Figure 1B. For each locality, sample number, data type present (mt, mtDNA; B, bacula), and corresponding voucher numbers or Genbank accession numbers (AF) are given. Specimens were obtained from the following institutions: Burke Museum of Natural History and Culture, Field Museum of Natural History, University of Idaho Vertebrate Collection (UIVC); Provincial Museum of Alberta, Edmonton (PMA); Royal British Columbia Museum, Victoria (RBCM); Connor Museum of Natural History, Washington State University (CMNH); University of Alberta Museum of Zoology, Edmonton (UAMZ); and the Canadian Museum of Nature, Ottawa (CMN). Haplotype designations correspond to those used in Figures 3 and 5, and frequency is indicated in parentheses. Alternatively, major mtDNA clade is given for some individuals (BASAL = 1, RUFI = 3, SIMU = 5, CANI = 6; Figs. 3, 5).

Locale	*n*	Data	Locality data and specimen information
1	1	B	Alberta, Canada, Castle River headwaters, *T. r. ruficaudus*: UAMZ 8174.
2	1	B	Alberta, Canada, Furman, *T. amoenus*-basal RM: PMA 87.17.2.
3	1	B	Alberta, Canada, Gibraltar Mt., *T. amoenus*-basal RM: UAMZ 8088.
4	1	B	Alberta, Canada, Gorge Creek, *T. amoenus*-basal RM: UAMZ 8098.
5	1	B	Alberta, Canada, Mines Lake, SE Beaver, +49.3, −114.283, *T. amoenus*-basal RM: PMA 87.17.4.
6	2	B	Alberta, Canada, Sheep River, *T. amoenus*-basal RM: UAMZ 8094–95.
7	1	mt	Alberta, Canada, Kananaskis Country, 2 km S Baril Creek on Hwy 940, +50.333, −114.617, *T. amoenus*-basal RM: AY120989 [L1].
8	1	mt	Alberta, Canada, Kananaskis Country, Wilkinson Creek, +50.217, −114.583, *T. amoenus*-basal RM: AY120990 [L7].
9	2	B, mt	British Columbia, Canada, 3 mi W Racehorse Pass, +49.782, −114.682, *T. amoenus*-basal RM: AY120981–82 [L3(2)].
10	2	mt	British Columbia, Canada, Andy Good Creek, below Mt. Ptolemy, +49.528, −114.642, *T. amoenus*-basal RM: AY120983–84 [L4(2)].
11	1	B, mt	British Columbia, Canada, Brisco, KM 19–20 Red Rock Rd, +50.762, −116.239, *T. amoenus*-basal CM: RBCM 19684 [L1].
12	5	B, mt	British Columbia, Canada, Church Creek Rd, +49.02, −117.43, *T. r. simulans*: AF401911, 18–20 [WI, WA, WI(2)], Salmo River, CMN 1008.
13	1	B, mt	British Columbia, Canada, Creston Valley, west side, Topaz Creek Forestry Rd, +49.167, −116.65, *T. amoenus*-basal CM: AY120970 [L12].
14	3	B, mt	British Columbia, Canada, Delphine Mine Trail, +50.438, −116.37, *T. amoenus*-basal CM: AY120976–78 [L1(3)].
15	6	B, mt	British Columbia, Canada, Giveout Creek FSR KM 9–10, +49.47, −117.33, *T. r. simulans*: AF401913–17, 37 [WA(6)].
16	3	B, mt	British Columbia, Canada, Gold Creek, Km 4.9 Gold Creek Rd, +49.439, −117.284, *T. r. simulans*: AF401910–11, 36 [WA(3)].
17	1	mt	British Columbia, Canada, Harvey Creek, +49.271, −114.7, *T. amoenus*-basal RM: RBCM 19905 [EG2].
18	1	B, mt	British Columbia, Canada, Junction of Lodgepole Rd and Windfall Mt. Rd, +49.293, −114.814, *T. amoenus*-basal RM: RBCM 19921 [EG2].
19	4	B, mt	British Columbia, Canada, Kishinena Creek, ~KM 99 Kishinena Rd, +49.036, −114.354, *T. amoenus*-basal RM: RBCM 19669–70, 74–75 [EG2(4)].
20	1	B, mt	British Columbia, Canada, Lead Queen Mt., east side, +50.719, −116.545, *T. amoenus*-basal CM, RBCM 19783 [BASAL].
21	10	B, mt	British Columbia, Canada, Paradise Mine Rd, *T. amoenus*-basal RM: head of basin +50.467, −116.308, RBCM 19746 [BASAL]; +50.468, −116.311, RBCM 19747 [BASAL]; old burn area, +50.48, −116.276, RBCM 19778–82 [BASAL(5)]; beginning of ascent +50.48, −116.271, AY120979–80 [L5, L1]; 10.7 km from Toby Creek, +50.473, −116.286, RBCM 19739 [BASAL].
22	20	B, mt	British Columbia, Canada, Rainy Ridge vicinity, Middle Kootenay Pass, +49.256, −114.402, *T. amoenus*-basal RM: RBCM 19877, 79, 81–82 [RUFI, EG2(3)], *T. r. ruficaudus*: AF401922–23, 25 [EC2, EG2, EB2], Middlepass Creek, +49.252, −114.404, *T. amoenus*-basal RM: RBCM 19886, 910 [EG2, RUFI], *T. r. ruficaudus*: AF401924, 26–35 [EB2, EG2(5), EB2, EG2(3), EC2].
23	3	B, mt	British Columbia, Canada, Sage Creek, ~3.5 km from Flathead Rd, +49.104, −114.454, *T. amoenus*-basal RM: AF401939–40, RBCM 19680 [EG2(2), EN2].
24	3	B, mt	British Columbia, Canada, Sage Creek, 21 km from Flathead Rd, +49.157, −114.267, *T. amoenus*-basal RM: RBCM 19679, 81, AF401938 [EG2(3)].
25	1	mt	British Columbia, Canada, Source of Akamina Creek, ~30 km W Wall Lake, +49.018, −114.078, *T. r. ruficaudus* AF401921 [EG2].
26	1	B, mt	British Columbia, Canada, Spring Creek Mine site, +50.476, −116.307, *T. amoenus*-basal CM: RBCM 19742 [BASAL].
27	8	B, mt	British Columbia, Canada, Todhunter Creek headwaters, +50.102, −114.745, *T. amoenus*-basal RM: RBCM 19894–01 [L1, BASAL, EG2, L1(2), BASAL, L1, BASAL].
28	8	B, mt	British Columbia, Canada, Hopeful Creek vicinity, *T. amoenus*-basal CM: +50.403, −116.186, RBCM 19770; +50.415, −116.19, RBCM 19771–72; +50.422, −116.191, RBCM 19773–77 [BASAL(8)].
29	12	B, mt	British Columbia, Canada, Mount Brewer vicinity, *T. amoenus*-basal CM: South Side, +50.422, −116.222, RBCM 19751–53; northeast Peak (unnamed), +50.393, −116.195, RBCM 19756–57; above Barsby Cabin, +50.391, −116.228, RBCM 19759, 64, 66–69; +50.397, −116.241, RBCM 19763 [BASAL(12)].

APPENDIX. Continued.

Locale	*n*	Data	Locality data and specimen information
30	3	mt	British Columbia, Canada, Stoddart Creek north ridge, +50.541, −115.993, *T. amoenus*-basal RM: RBCM 19748–49; +50.555, −115.999, RBCM 19784 [BASAL(3)].
31	1	B, mt	British Columbia, Canada, Toby Creek, 1.5 km SW Panorama Ski Area, +50.448, −116.256, *T. amoenus*-basal CM: RBCM 19750 [BASAL].
32	2	B, mt	British Columbia, Canada, Wynndel, Darcie Shepard Farm, +49.158, −116.533, *T. amoenus*-basal CM: AY120985–86 [L1, L6].
33	3	B	British Columbia, Canada, Kootenay Pass, *T. r. simulans*: CMN 41277, 82, 86.
34	1	mt	Idaho, Benewah Co., 10 mi N Potlatch, base of Mineral Mt., +47.053, −116.87, *T. r. simulans*: AF401784 [WD].
35	2	B, mt	Idaho, Boundary Co., Jeru Creek, 17 mi N Sandpoint, +48.513, −116.583, *T. r. simulans*: AF401783, 864 [WH, WA].
36	8	B, mt	Idaho, Clearwater Co., 0.7 mi E Mouth, Weitas Creek, +46.642, −115.424, *T. r. simulans*: AF401818–25 [EP, WA, EP, ER, WA, EP, ET, WA].
37	3	B, mt	Idaho, Clearwater Co., 19 mi N Kelly Forks, Rawhide Creek, +46.911, −115.065, *T. r. simulans*: AF401811–13 [EP, EO, EV].
38	1	B	Idaho, Clearwater Co., 2 mi W 3 mi E Weippe, *T. r. simulans*: CMNH 8179.
39	5	B, mt	Idaho, Clearwater Co., 38 mi NE Pierce, Cayuse Landing, +46.668, −115.067, *T. r. simulans*: AF401833–37 [EM(4), EA].
40	2	B, mt	Idaho, Clearwater Co., 3 km NE mouth Nork Fork Clearwater River, Dworshak Dam, +46.519. −116.307, *T. a. canicaudus*: UIVC JMG57–58 [CE(2)].
41	5	mt	Idaho, Clearwater Co., 4 mi N Elk River, +46.823, −116.177, *T. r. simulans*: AF401856–60 [WF, WA, EN, WA(2)].
42	4	mt	Idaho, Clearwater Co., 4.5 mi E Teaken, Freeman Creek, +46.57, −116.27, *T. r. simulans*: AF401894–97 [WB(4)].
43	1	B, mt	Idaho, Clearwater Co., 6 mi S Pierce, Jim Brown Creek, +46.386, −115.796, *T. r. simulans*: UIVC JMG33 [EP].
44	5	B. mt	Idaho, Clearwater Co., 9 mi NW Kelly Forks, Mush Saddle, +46.753, −115.369, *T. r. simulans*: AF401884–88 [EP, ES, WA(2), ED].
45	4	B, mt	Idaho, Clearwater Co., Idaho, 1.4 mi E Kelly Forks, Junction Creek, +46.719, −115.233, *T. r. simulans*: AF401814–17 [ED, EA, EC, EP].
46	4	B, mt	Idaho, Clearwater Co., Dworshak Reservoir, near Dent Acres, +46.62, −116.23, *T. r. simulans*: UIVC JMG27–28 [WA(2)], *T. a. canicaudus*: JRD159–160 [CA, CANI].
47	5	B, mt	Idaho, Idaho Co., 10.5 mi SE Grangeville, FR648A, Cougar Mt., +45.84, −115.83, *T. r. ruficaudus*: AF401898–00 [EI(3)], UIVC JRD19, 21 [RUFI(2)].
48	5	B, mt	Idaho, Idaho Co., 11 mi NE Lowell, Split Creek pack bridge, +46.231, −115.412, north bank, *T. r. simulans*: UIVC JMG29 [EA], south bank, *T. r. ruficaudus*: AF401848–49, 92–93 [EP, EI, EP, EI].
49	7	B, mt	Idaho, Idaho Co., 13 mi S confluence Lochsa/Selway, +45.968, −115.593, *T. r. ruficaudus*: AF401759–65 [EH, EI(4), EK, EI].
50	5	B, mt	Idaho, Idaho Co., 18 mi E Pierce, Rocky Ridge Lake, +46.439, −115.489, *T. r. simulans*: AF401826–30 [EQ, EZ, ER, EP(2)].
51	1	B	Idaho, Idaho Co., 20 mi E Lowell, Stanley Hot Springs, *T. r. ruficaudus*: CMNH 80-93.
52	1	B, mt	Idaho, Idaho Co., 25 km N Elk City, FR443, +46.002, −115.395, *T. r. ruficaudus*: UIVC JMG91 [EJ2].
53	5	B, mt	Idaho, Idaho Co., 30 mi E Pierce, Twelve-Mile Saddle, +46.510, −115.154, *T. r. simulans*: AF401843–47 [ED, EP(2), EC, EP].
54	5	B, mt	Idaho, Idaho Co., 30 mi NE Lowell, Eagle Mt. pack bridge, +46.430, −115.129, north bank, *T. r. simulans*: AF401831 [EP], south bank, *T. r. ruficaudus*: AF401832, 89–91 [EL, EI(3)].
55	7	B, mt	Idaho, Idaho Co., 40 mi E Pierce, Indian Post Office, +46.540, −114.989, *T. r. simulans*: UIVC JMG153–54 [EM2, EL2], AF401838–42 [EA2(2), EE, EZ, EA].
56	4	B, mt	Idaho, Idaho Co., Elk Summit/Hoodoo Lake, +46.345, −114.64, *T. r. ruficaudus*: UIVC JMG74–75, 77, 80 [EA, EI, EP, EZ].
57	3	B, mt	Idaho, Idaho Co., Lolo Pass/Elk Meadows, +46.635, −114.578, *T. r. ruficaudus*: AF401766–68 [EF2, EB(2)].
58	16	B, mt	Idaho, Idaho Co., Warm Springs Trail Head, +46.461, −115.018, north bank, *T. r. simulans*: UIVC JMG150, 55, 57 [EL2, RUFI, SIMU] UIVC JMS298, south bank, *T. r. ruficaudus*: AF401850–53, [EP(2), EI, EF] UIVC JMS301, 05–06, UIVC JMG143–44, 46, 48–49 [EK2, EP, EK2, EI(2)].
59	3	B, mt	Idaho, Kootenai Co., 12.5 mi N Enaville, +47.708, −116.377, *T. r. simulans*: AF401861–63 [WG, WA(2)].
60	2	B, mt	Idaho, Latah Co., 4 mi SE Moscow, Paradise Ridge, +46.69, −116.971, *T. r. simulans*: AF401854–55 [ED(2)].
61	12	B, mt	Idaho, Latah Co., Idaho, Latah Co., Moscow vicinity, 8 mi NE, Moscow Mt., +46.808, −116.9, *T. r. simulans*, AF401800–10 [WC, WA(5), WE, WA(4)]; 6 mi E Moscow, Seversen, Wallen Rd, AF401785 [WA].
62	5	B, mt	Idaho, Shoshone Co., 8.2 mi E Avery, +47.225, −115.606, *T. r. simulans*: AF401869–73 [EP(3), WA(2)].
63	3	B	Idaho, Shoshone Co., NE Clarkia, *T. r. simulans*: 15 mi E, 2 mi N, CMNH 82100; 17 mi E, 2 mi N, CMNH 82101; 8 mi E, 1 mi N, CMNH 8298.

APPENDIX. Continued.

Locale	*n*	Data	Locality data and specimen information
64	10	B, mt	Montana, Beaverhead Co., 8 km E Lost Trail Pass, Trail Creek, +45.73, −113.90, *T. r. ruficaudus*: UIVC JMG59, 61, 63–64, 66, 72 AF401906–09 [EI(2), EG2(2), EI, RUFI, EF2, EI(2), EJ].
65	7	B, mt	Montana, Beaverhead Co., Pioneer Mts., *T. r. ruficaudus*: 4 mi NW Comet Mt., FR 484, +45.45, −113.08, AF401786–89 [EI(4)]; 4 km E Table Mt., +45.483, −113.10, AF401903 [EI]; 6 km SE Saddleback Mt., +45.417, −112.90 AF401904–5 [EI(2)].
66	5	B, mt	Montana, Beaverhead Co., Selway Mts., Bloody Dick Creek, FR1818, +45.15, −113.50, *T. r. ruficaudus*: AF401945–49 [EI(3), EI2, EI].
67	1	mt	Montana, Beaverhead, Lower Miner Lake, 20 km W Jackson, +45.32, −113.58, *T. r. ruficaudus*: AF401902 [EI].
68	16	B, mt	Montana, Flathead Co., 12 km NNE Whitefish, +48.506, −114.248, *T. r. simulans*: AF401876–83 [WA, EG2, WA(2), EG2, WA, EG2, WA], UIVC JMG126–33 [EG2(2), WA(3), WJ, WA(2)].
69	13	B, mt	Montana, Flathead Co., 35 km W Whitefish, 2 km S Good Creek, +48.42, −114.825, *T. r. simulans*: UIVC JMG108, 13–14, 16–19 [WA(7)], *T. amoenus*-basal RM: UIVC JMG107, 09–12, 15 [EG2(6)].
70	10	B, mt	Montana, Flathead Co., 8 km E Hungry Horse, Desert Mt., +48.393, −113.945, *T. r. ruficaudus*: UIVC JMG134–42, 59 [EG2, E02, EG2, RUFI, EG2(5), RUFI].
71	1	mt	Montana, Flathead, near Essex along Highway 2, +48.28, −113.61, *T. r. ruficaudus*: AF401901 [ED2].
72	4	B, mt	Montana, Granite Co., Brewster Creek, Sliderock Mt., +46.586, −114.578, AF401769–72 [EG2(3), EE2].
73	4	B, mt	Montana, Lincoln Co., 4 mi S Libby, Flower Creek, +48.343, −115.601, *T. r. simulans*: UIVC JMS199, 216–18 [WA(2), SIMU, WA].
74	5	B, mt	Montana, Lincoln Co., N Libby, +48.4, −115.55, *T. amoenus*-basal CM: AY121062–66 [L11, L10, L9, L1(2)].
75	4	B, mt	Montana, Missoula Co., S Lolo, +46.686, −114.077, *T. r. ruficaudus*: AF401773–76 [EP, EI, EG(2)].
76	2	B, mt	Montana, Rivalli Co., 4 mi W Florence, +46.62, −114.15, *T. r. ruficaudus*: AF401779–80 [ED, EI].
77	2	B, mt	Montana, Rivalli Co., Bass Creek Campground, +46.576, −114.138, *T. r. ruficaudus*: AF401777–78 [EU(2)].
78	2	mt	Montana, Sanders Co., 2 km N Beaver Creek, 5 km E Sex Peak, 20 km NW Thompson Falls, +47.037, −115.5, *T. a. canicaudus*: UIVC JMG160 [CA], *T. ruficaudus*: UIVC JMG161 [EP].
79	2	B, mt	Washington, Whitman Co., Steptoe Butte Summit, UIVC JRD161–62 [CB(2)].
80	16	B, mt	Washington, Douglas Co., Waterville vicinity, *T. a. canicaudus*: 4 mi S Waterville, Badger Mt., +47.61, −120.13 UIVC JMG39–49 [CG(4), CH(3), CG, CH, CA, CC]; 4 mi W Waterville, Pine Canyon, +47.65, −120.15, UIVC JMG34–38 [CH(5)].
81	2	B, mt	Washington, Ferry Co., 5 km E Curlew Lake, Herron Creek Rd, +48.7, −118.67, *T. amoenus*-basal CM: AY120996–97 [L1, L8].
82	8	B	Washington, Ferry Co., Kettle River Range, *T. amoenus*-basal CM: 1 mi N Sherman Pass, T36N, R34E, S24, CMNH 983737; 17 mi W, 1 mi S Kettle Falls, CMNH 8255–56; 0.9 mi N, 1 mi W Copper Butte, CMNH 983743–44; 2.8 mi W, 5 mi N Sherman Pass, N Fork O'brien Cr, CMNH 983738, 40–41.
83	16	B, mt	Washington, Whitman Co., Kamiak Butte vicinity, *T. a. canicaudus*: 4 mi N Albion, Smoot Hill Ecological Reserve, +46.82, −117.21, AF401781–82, 91–99 [CF(11)], CMNH 8062, 64, 8155, 8159; Kamiak Butte, CMNH 8078.
84	7	B, mt	Washington, Lincoln Co., 1.5 mi SE Lillenthal Mt., +47.88, −118.22, *T. a. canicaudus*: UIVC JMG50–56 [CA, CC, CA(3), CD(2)].
85	3	mt	Washington, Okanogan Co., off FS 4953, FS 50, +48.82, −119.03, *T. amoenus*-basal CM: AY120957–59, [L1, L2, L1].
86	2	B	Washington, Pend Oreille Co., Little Ruby Creek, 6 mi W Blueside, *T. r. simulans*: CMNH 8173–74.
87	17	B, mt	Washington, Pend Oreille Co., Sullivan Creek Drainage, *T. r. simulans*: Gypsy Creek Basin, CMNH 8356; Gypsy Peak, CMNH 81574; Leola Creek, CMNH 80698–99, 701, CMNH 8357; Creek Pass, CMNH 983910,13; Round Top Mt., CMNH 983914–15; Shedroof Mt., CMNH 82474; Sullivan Lake, +48.85, −117.18, CMNH 8094, AF401865–68 [WA(4)], *T. amoenus*-basal CM: UIVC JMS207 [L1].
88	3	B	Washington, Stevens Co., Churchill Mt. vicinity, *T. amoenus*-basal CM: CMNH 82505–06; 0.7 mi W, 0.8 mi N Elbow Lake Campground, CMNH 82495.
89	2	B	Washington, Spokane Co., Mt. Spokane, *T. r. simulans*: CMNH 82490–91.
90	7	B, mt	Washington, Spokane Co., Turnbull NWR, 7 km S Cheney, +46.426, −117.566, *T. a. canicaudus*: UIVC JMG101–06 [CA(6)]; 16 mi S, 6 mi W Cheney, CMNH 8081.

T. amoenus AY120971 (British Columbia), AF147630 (California), AY121067 (Idaho), AY121003 (Idaho), AY121081 (Montana), AY120969 (Oregon), AY121071 (Oregon), AF147632 (Washington), AY121041 (Washington); *T. bulleri* AF147634; *T. canipes* AF147635; *T. cinereicollis* AF147636; *T. dorsalis* AF147641; *T. durangae* AF147642; *T. merriami* AF147644; *T. minimus* AF147645 (Alberta), AF147646 (California), AF147649 (Manitoba), AF147650 (Utah), AY120942 (Wyoming); *T. obscurus* AF147653; *T. panamintimus* AF147656; *T. quadrimaculatus* AF147657; *T. quadrivittatus* AF147658; *T. rufus* AF147662; *T. senex* AF147665; *T. sibiricus* AF147666; *T. siskiyou* AF147668; *T. striatus* AF147670; *T. townsendii* AF147674.